GRINENKO-SHUL’GA MECHANISM OF FAST CHARGED PARTICLE DEFLECTION USING BENT CRYSTALS

Igor KYRYLLIN

Akhiezer Institute for Theoretical Physics of National Science Center
”Kharkiv Institute of Physics and Technology”,
Kharkiv, Ukraine

June 10, 2025

Scattering of charged particles in a crystal

Robinson M. T., Oen O. S., Holmes D. K. Computer studies of anomalous penetration of Cu recoil atoms in Cu crystal. Proc. of Conference «Bombardment Ionique». CNRS. Paris. 1962. P. 105.
Robinson M. T., Oen O. S. Computer studies of the slowing down of energetic atoms in crystals. Phys. Rev. 1963. Vol. 132, No. 6. P. 2385.

Cu^{+}, E=1-10 keV

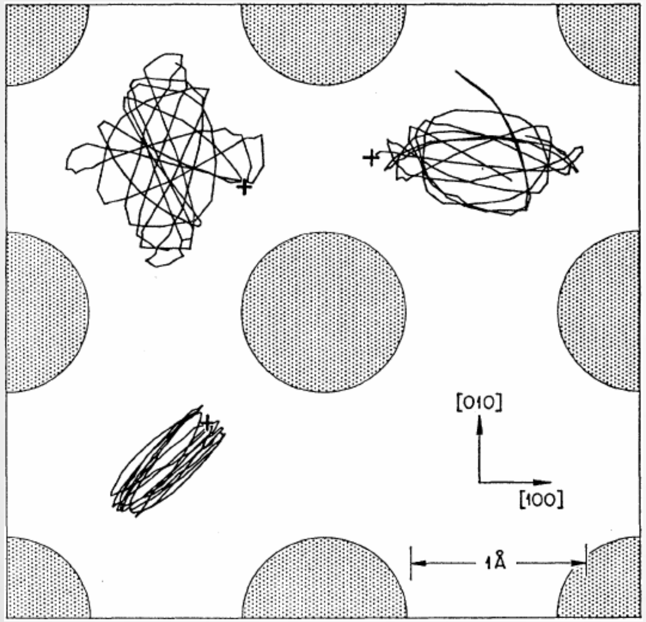

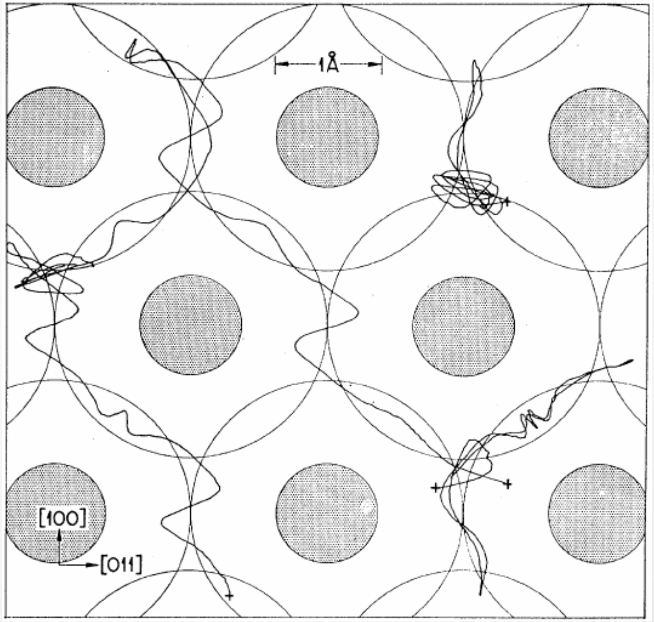

Lindhard J. Influence of crystal lattice on motion of energetic charged particles. Mat. Fys. Medd. Dan. Vid. Selsk. 1965. Vol. 34, No. 14. P. 1–64.

Approximation of continuous potential

$$\frac{d}{dt}\frac{m\mathbf{v}}{\sqrt{1-v^2/c^2}} = -q\nabla\Phi_c(\mathbf{r})$$

$$\Phi_c(\mathbf{r})=\sum_n \Phi_a(\mathbf{r}-\mathbf{r}_n)$$

$$\Phi(\boldsymbol{\rho})=\frac{1}{L}\int_{-\infty}^{\infty} dz\,\Phi_c(\boldsymbol{\rho},z)$$

$$\ddot{\boldsymbol{\rho}} = -\frac{c^2 q}{E_\parallel}\frac{\partial}{\partial\boldsymbol{\rho}}\Phi(\boldsymbol{\rho})$$

$$E_\parallel = c\sqrt{p_\parallel^2+(mc)^2}$$

Lindhard J. Influence of crystal lattice on motion of energetic charged particles. Mat. Fys. Medd. Dan. Vid. Selsk. 1965. Vol. 34, No. 14. P. 1–64.

Potential of crystal atomic strings

Si <100>

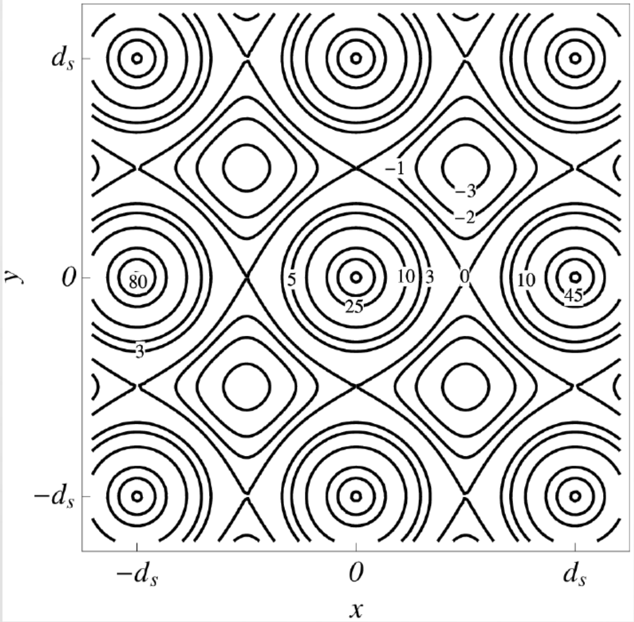

Si <111>

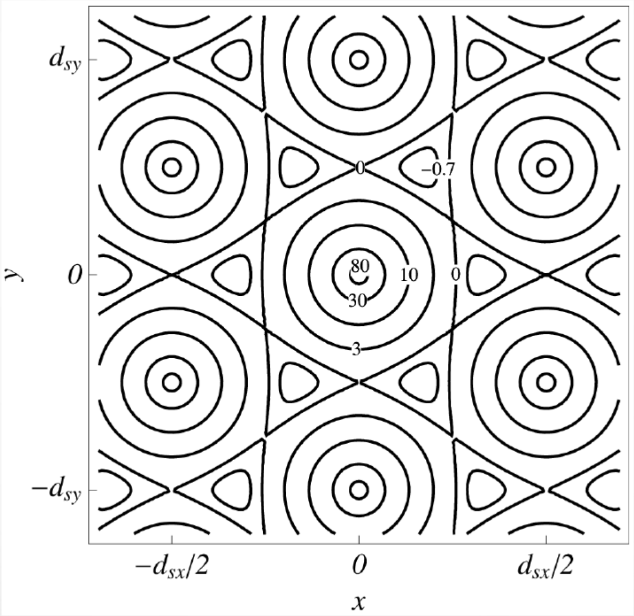

Si <110>

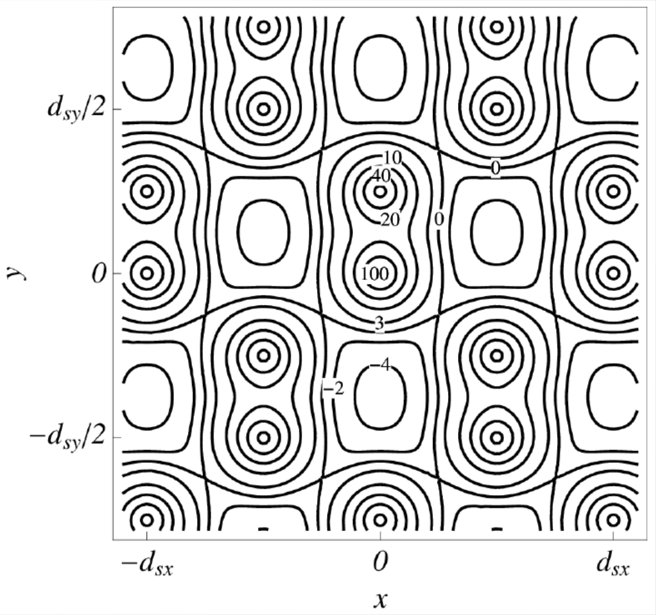

Potential of crystal atomic strings

Si <100>

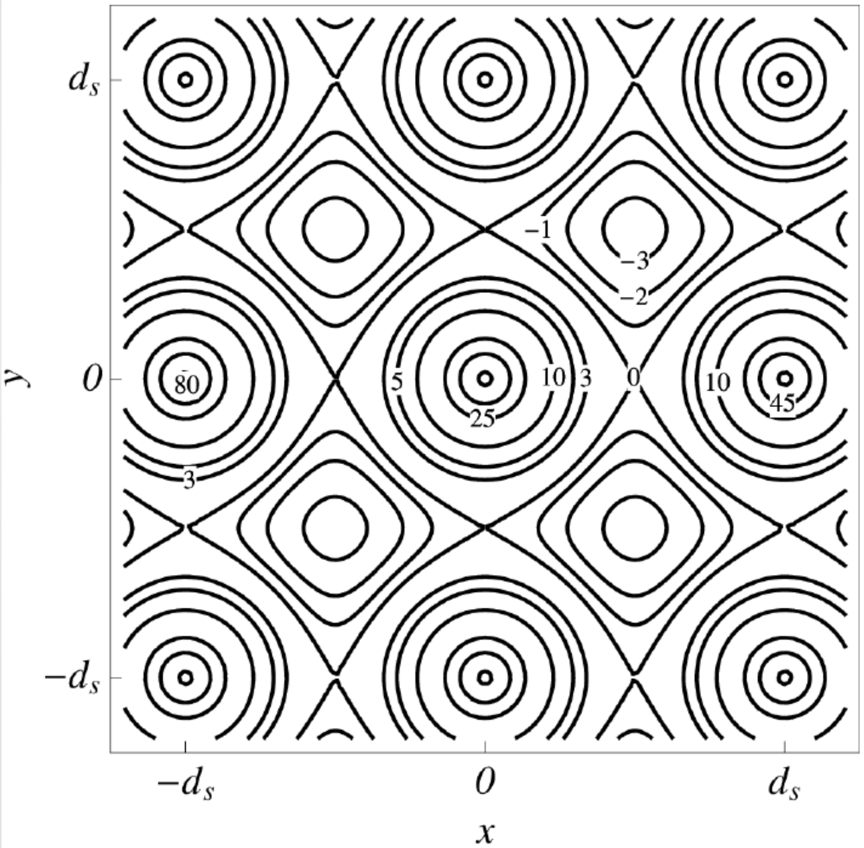

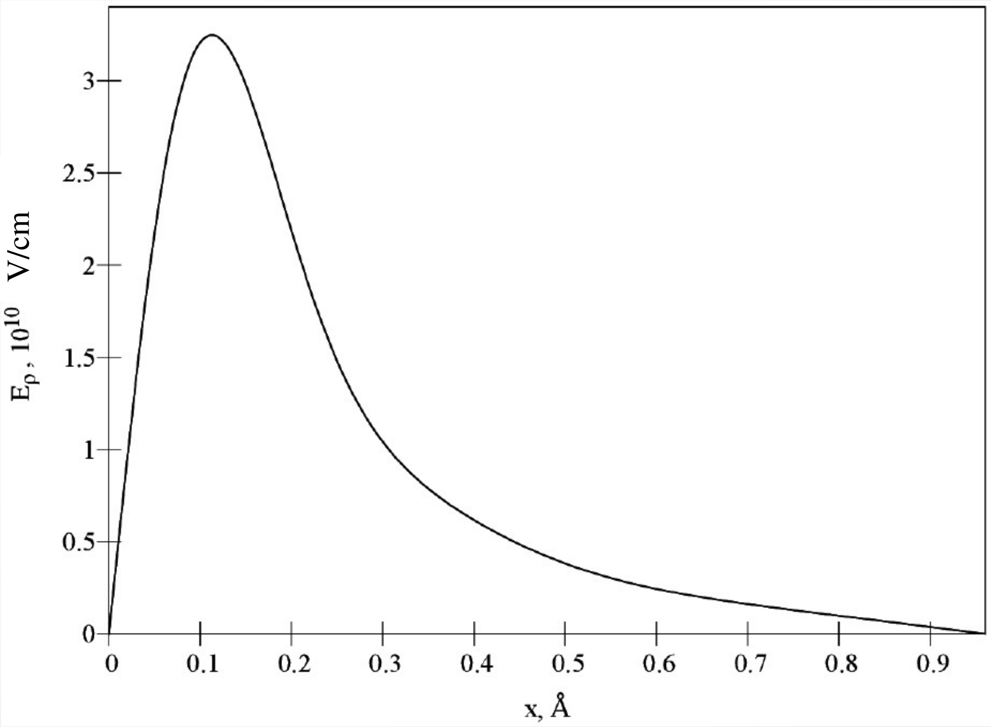

$E_{str} \sim 10^{10}$ V/cm

Potential of crystal atomic planes

Si (100)

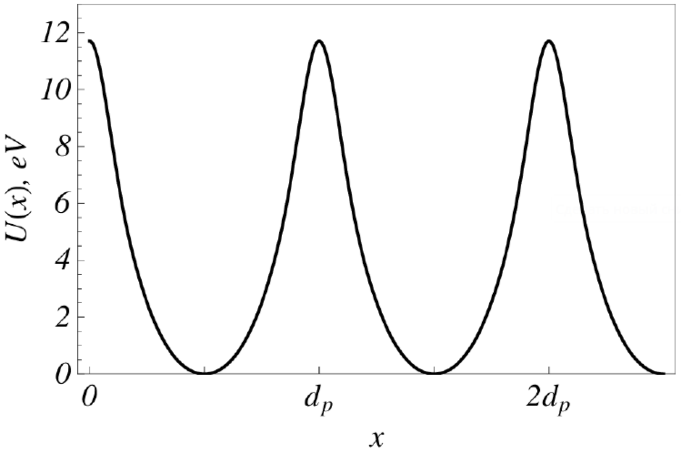

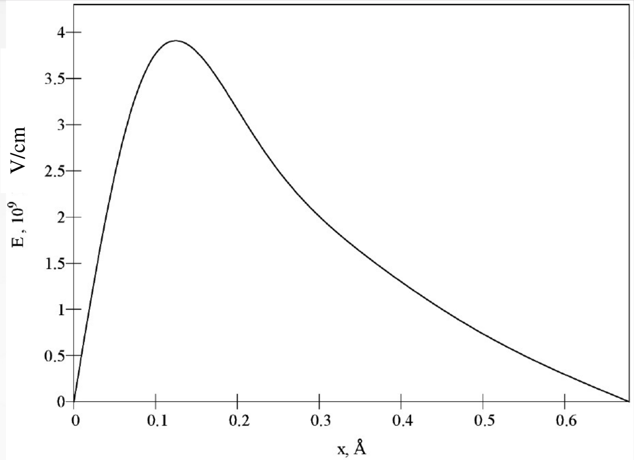

$E_{str} \sim 10^{10}$ V/cm
$E_{pl} \sim 10^{9}$ V/cm

Si (110)

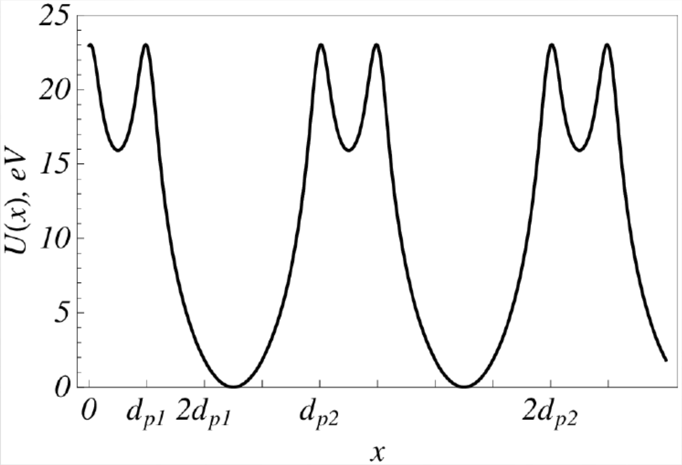

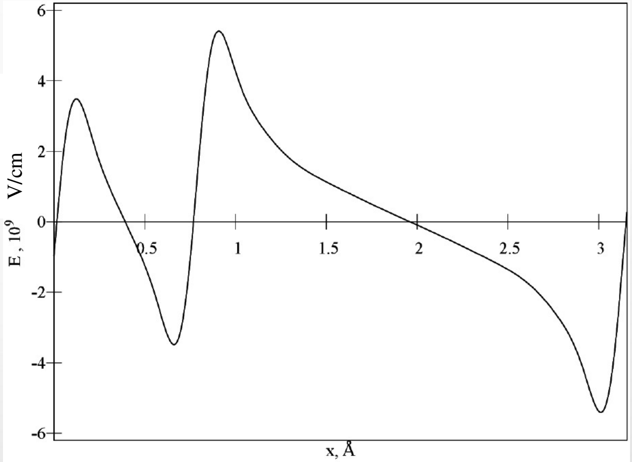

Regimes of motion in a crystal

$\psi_x \approx \psi_y < \psi_c$

$\psi_x < \theta_c , \psi_y \gg \psi_c$

$\psi_x > \theta_c , \psi_y \gg \psi_c$

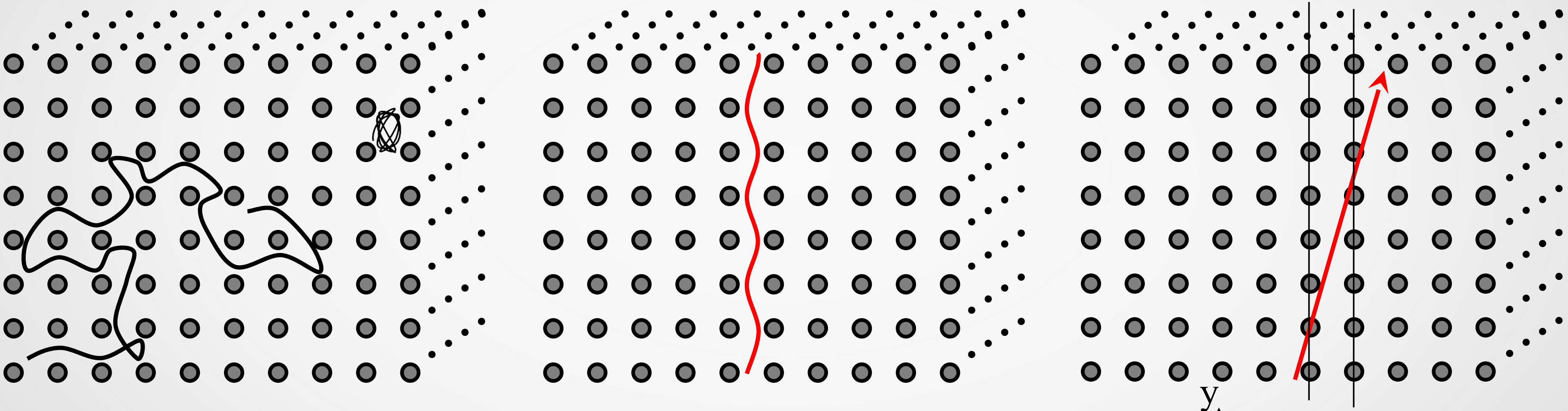

$$v_z \approx c , \qquad \psi_x = \frac{v_x}{c} , \qquad \psi_y = \frac{v_y}{c} , \qquad \psi_c \approx 2\theta_c \sim 10^{-5}$$

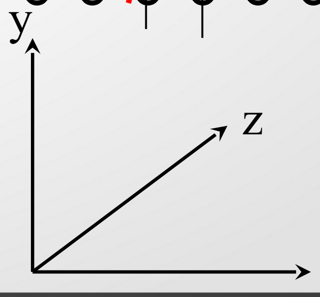

Bent crystals and magnetic deflection systems

Magnets

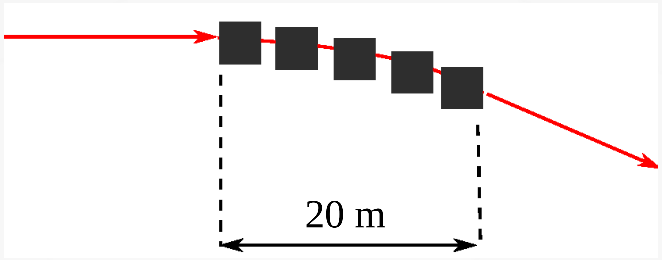

Bent crystal

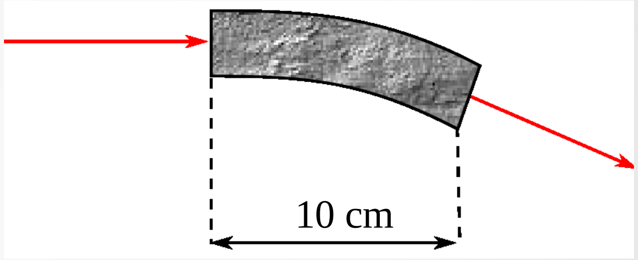

$E_{str} \sim 10^{10}$ V/cm
$E_{pl} \sim 10^{9}$ V/cm

Advantages of bent crystals in comparison with magnetic deflection systems:

- Small size
- do not need electricity consumption
- do not need cooling

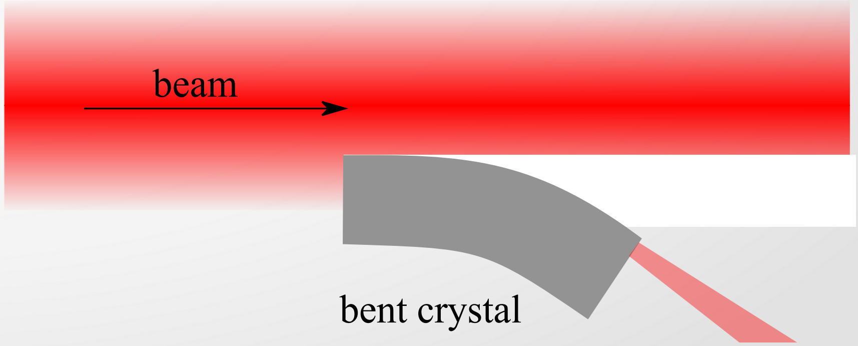

Mechanisms of deflection

Planar channeling

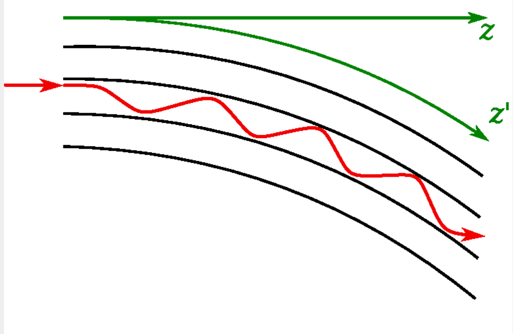

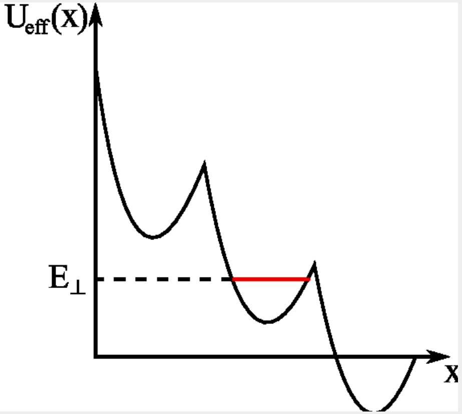

Tsyganov E. N. Fermilab TM-682, TM-684. 1976.

Volume reflection

Taratin A. M., Vorobiev S. A. Phys. Lett. A. 1986. Vol. 115, No. 8. P. 398–400.

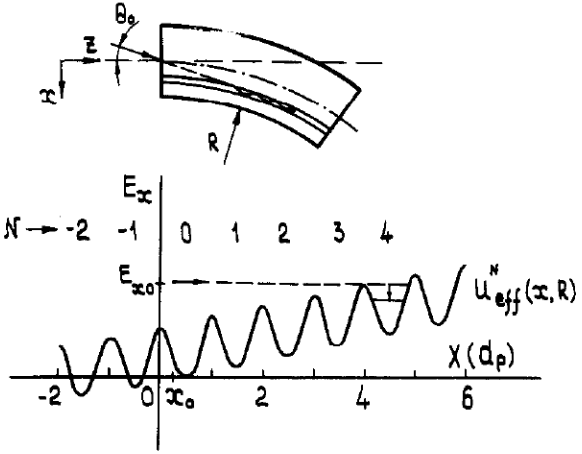

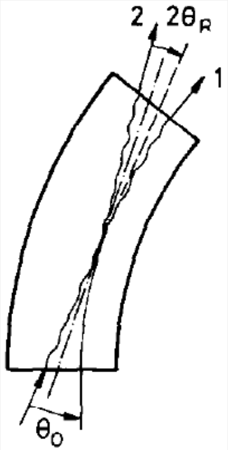

Stochastic deflection

Grinenko A. A., Shul'ga N. F. J. Exp. Theor. Phys. Lett. 1991. Vol. 54. P. 524–528.

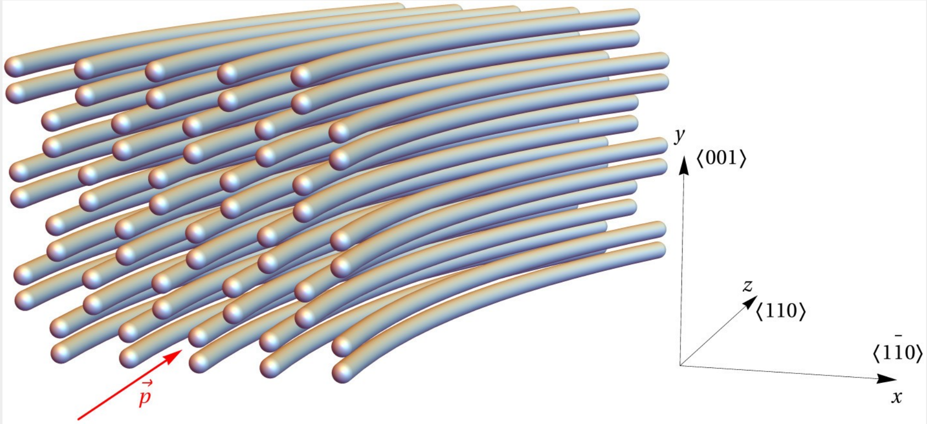

Planar channeling

Tsyganov E. N. Fermilab TM-682, TM-684. 1976.

$$\psi_x < \theta_c, \psi_y \gg \psi_c$$

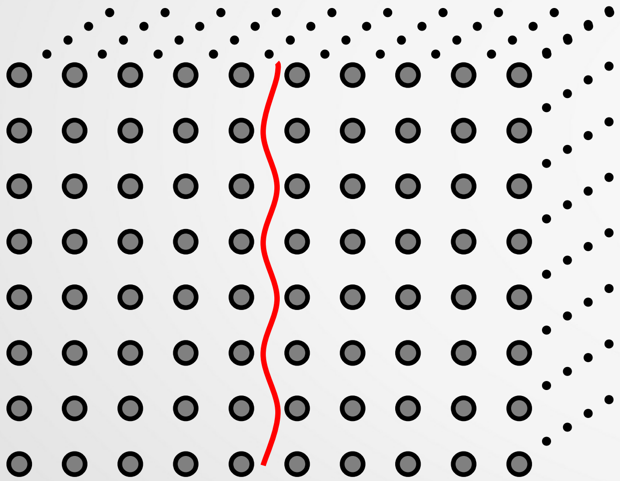

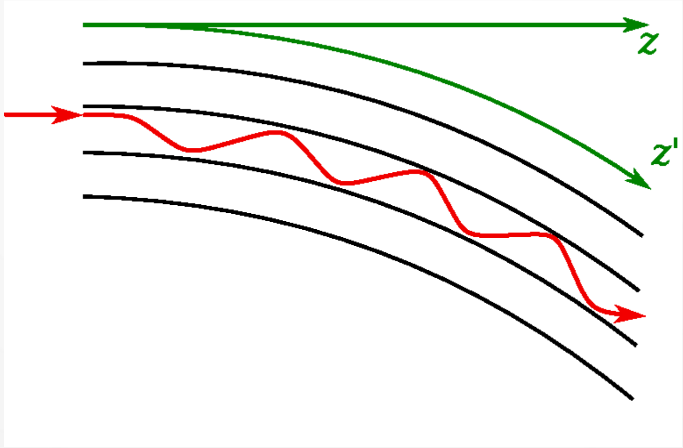

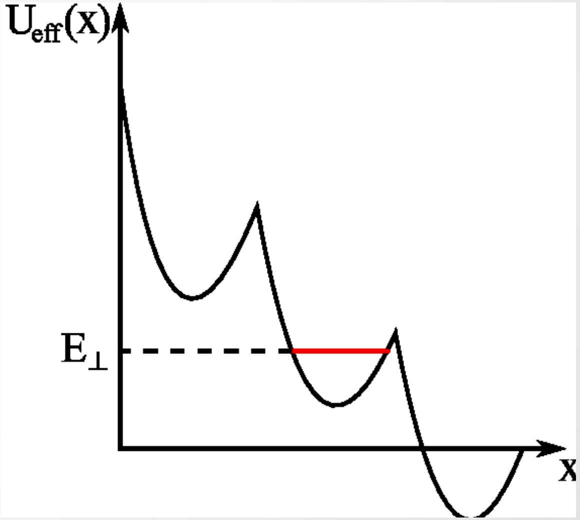

Planar channeling

Tsyganov E. N. Fermilab TM-682, TM-684. 1976.

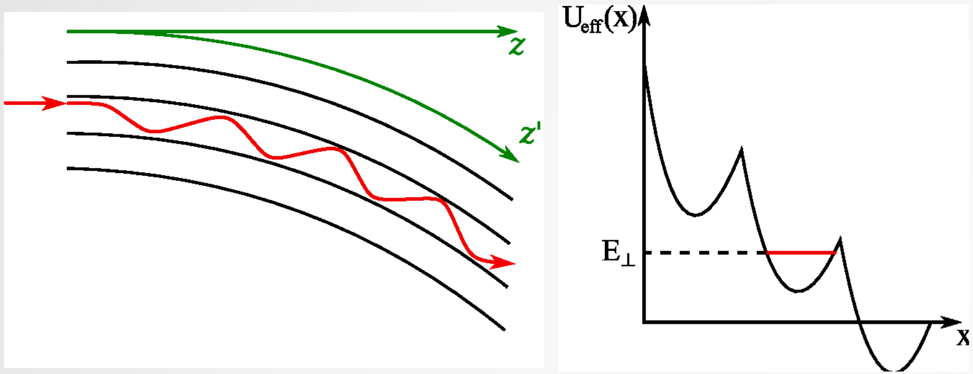

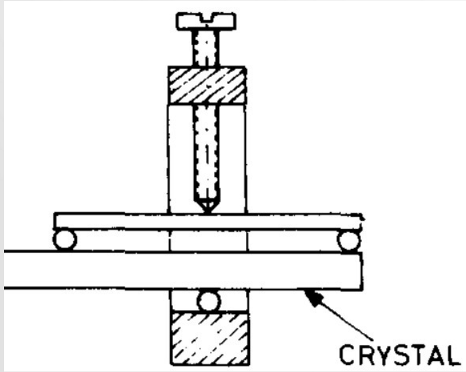

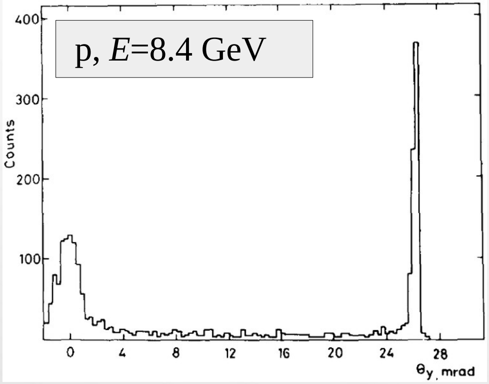

Таратин А. М., Цыганов Э. Н., Воробьев С. А. Поворот пучков заряженных частиц изогнутым монокристаллом. Численный эксперимент. Письма в ЖТФ. 1978. Т. 4. С. 947–950.
Tarantin A. M., Tsyganov E. N., Vorobiev S. A. Computer simulation of deflection effects for relativistic charged particles in a curved crystal. Phys.Lett. A. 1979. Vol. 72, No. 2. P. 145–146.

p, *E*=1 GeV, a) *R*=0,29 cm, b) *R*=0,112 cm

Elishev A. F., Filatova N. A., Golovatyuk V. M. et al. (I.A. Grishaev, G.D. Kovalenko, B.I. Shramenko) Steering of charged particle trajectories by a bent crystal. Phys. Lett. B. 1979. Vol. 88, No. 3-4. P. 387–391.

Volume reflection

Taratin A. M., Vorobiev S. A. Phys. Lett. A. 1986. Vol. 115, No. 8. P. 398–400.
Taratin A. M., Vorobiev S. A. Nucl. Instrum. Meth. B. 1987. Vol. 26, No. 4. P. 512–521.
Taratin A. M., Vorobiev S. A. Phys. Lett. A. 1987. Vol. 119, No. 8. P. 425–428.

$$E_x = \frac{pv\theta_x^2}{2} + U_{eff}(x, R)$$

$$U_{eff}(x, R) = U(x) + pv\frac{x}{R}$$

$$\psi_x > \theta_c ,\ \psi_y \gg \psi_c$$

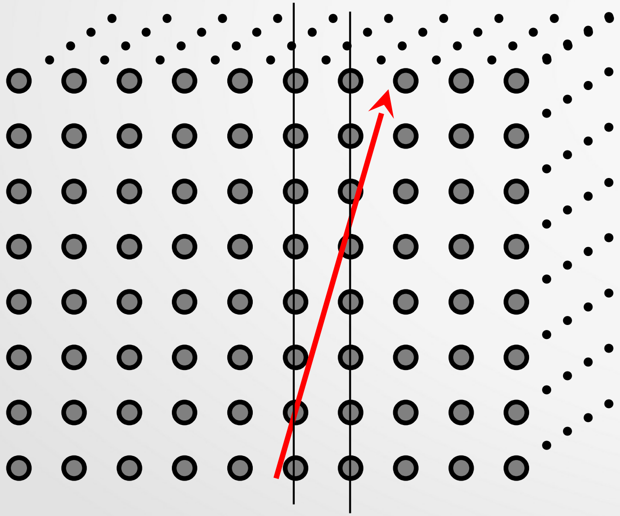

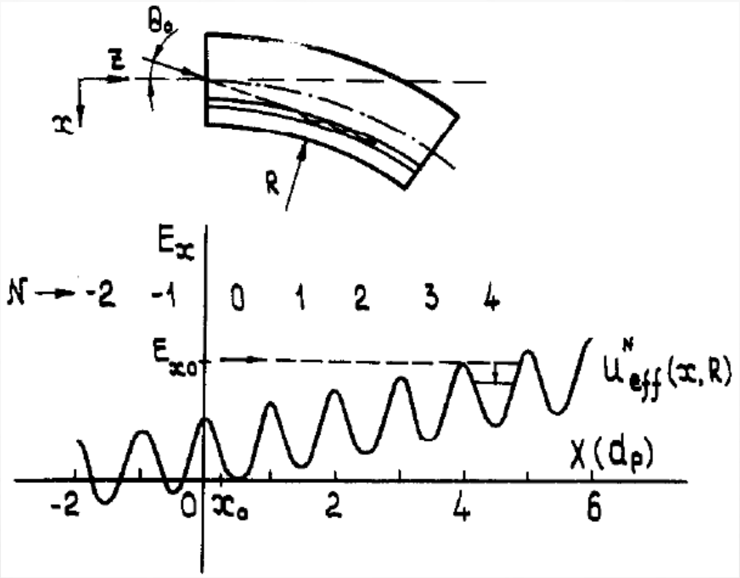

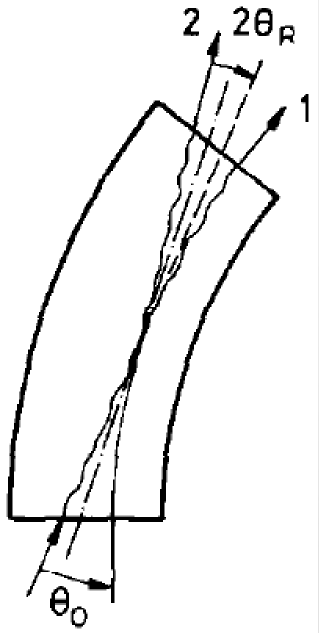

Stochastic deflection

Grinenko A. A., Shul’ga N. F. J. Exp. Theor. Phys. Lett. 1991. Vol. 54. P. 524–528.
Greenenko A. A., Shul’ga N. F. Nucl. Instrum. Meth. B. 1994. Vol. 90, No. 1-4. P. 179–182.
Shul’ga N. F., Greenenko A. A. Phys. Lett. B. 1995. Vol. 353, No. 2. P. 373–377.

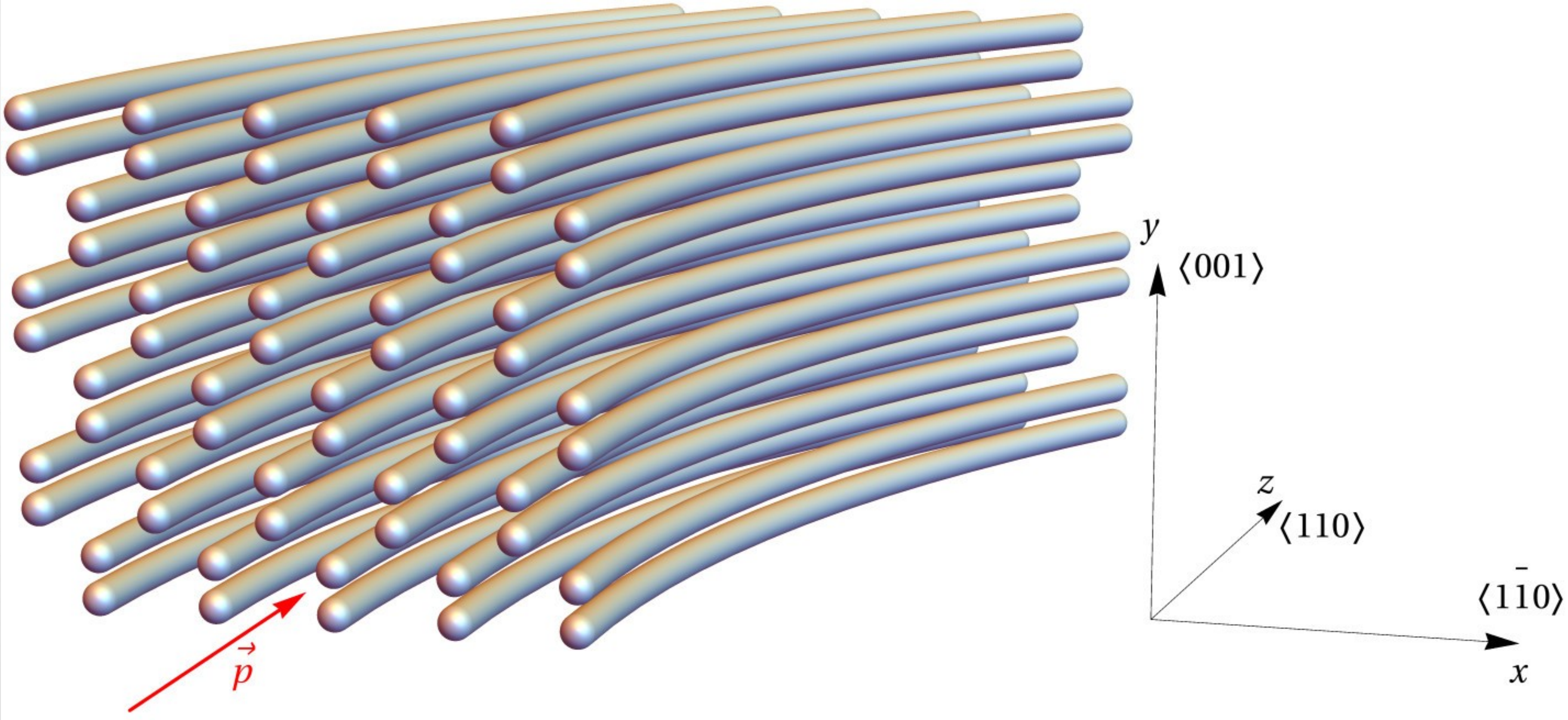

Dynamical chaos in the motion of fast charged particles in crystals

1. Yu. L. Bolotin, V. Yu. Gonchar, V.I. Truten’, N.F. Shul’ga, Ukr. Fiz. Zh. 31 (1986) 14 (in Russian); Dokl. Akad. Nauk SSSR 296 (1987) 1104 (in Russian).
2. N.F. Shulga, Yu.L. Bolotin, V.Yu. Gonchar, V.I. Truten’. Dynamical chaos in the motion of fast charged particles in crystals // Physics Letters A. Elsevier, 1987. Vol. 123, № 7. P. 357–360.
3. Shul’ga N.F., Laskin N.V., V.I. Truten’. Dynamical chaos in the motion of fast charged particles in crystals // Nucl. Instrum. Meth. B. 1990. Vol. 48, № 1. P. 174–180.

$$U(\boldsymbol{\rho}) = \frac{1}{T}\int dz \sum_k u(\boldsymbol{r}-\boldsymbol{r}_k)$$

$$\ddot{\boldsymbol{\rho}} = -\frac{1}{\mathscr{E}_\parallel}\frac{\partial}{\partial \boldsymbol{\rho}} U(\boldsymbol{\rho}), \quad \boldsymbol{\rho} = (x, y)$$

$$\mathscr{E}_\perp = \tfrac{1}{2}\mathscr{E}\dot{\boldsymbol{\rho}}^2 + U(\boldsymbol{\rho})$$

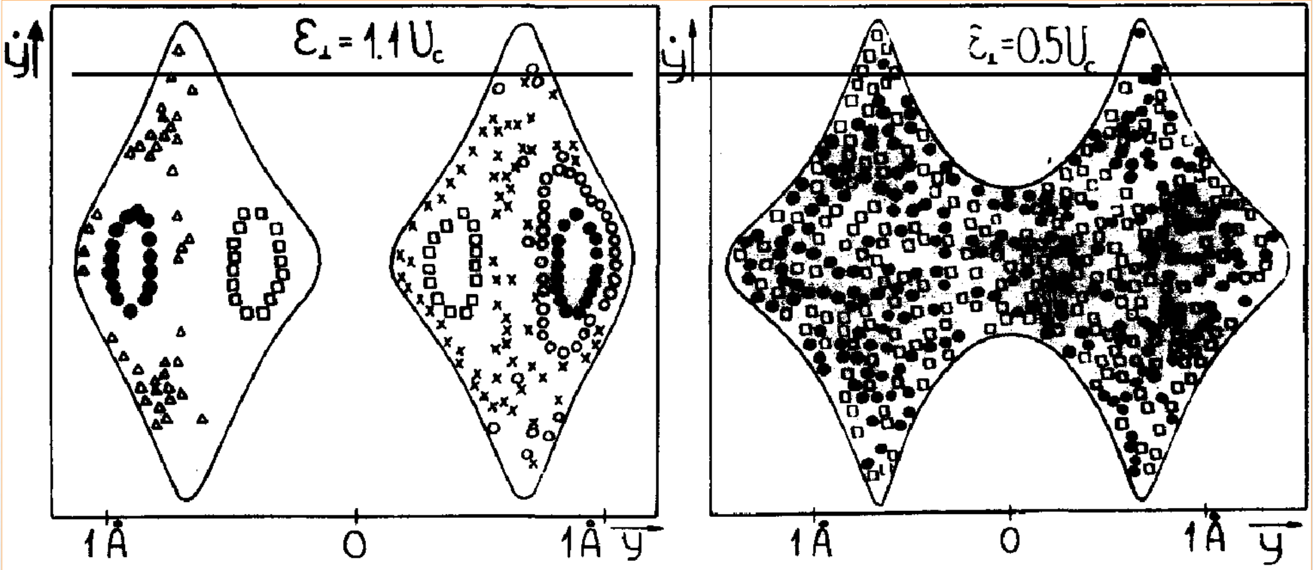

Fig. 2. The Poincaré cross sections for electrons channeled in the ⟨110⟩ direction in Si.

Dynamic chaos in the motion of charged particles through a crystal

Akhiezer A.I., V.I. Truten’, Shul’ga N.F. Dynamic chaos in the motion of charged particles through a crystal // Phys. Rep. (Review Section of Physics Letters). 1991. Vol. 203, № 5. P. 289–343.

$$\boldsymbol{\xi} = \boldsymbol{r}^{(1)} - \boldsymbol{r}^{(2)}, \qquad \boldsymbol{\eta} = \boldsymbol{p}^{(1)} - \boldsymbol{p}^{(2)}$$

$$\dot{\boldsymbol{\xi}} = \boldsymbol{\eta}, \qquad \dot{\boldsymbol{\eta}} = -\hat{S}(t)\boldsymbol{\xi}$$

$$S_{ij} = \partial^2 U / \partial r_i \, \partial r_j \big|_{\boldsymbol{r}=\boldsymbol{r}^{(1)}(t)}$$

$$\begin{pmatrix} \dot{\boldsymbol{\xi}} \\ \dot{\boldsymbol{\eta}} \end{pmatrix} = \hat{\Gamma} \begin{pmatrix} \boldsymbol{\xi} \\ \boldsymbol{\eta} \end{pmatrix}$$

$$\hat{\Gamma} = \begin{pmatrix} \hat{0} & \hat{I} \\ -\hat{S} & \hat{0} \end{pmatrix}$$

$$\det(\hat{\Gamma}) = \det\begin{pmatrix} -\lambda & 0 & 1 & 0 \\ 0 & -\lambda & 0 & 1 \\ -\partial^2 U/\partial x^2 & -\partial^2 U/\partial x\,\partial y & -\lambda & 0 \\ -\partial^2 U/\partial y\,\partial x & -\partial^2 U/\partial y^2 & 0 & -\lambda \end{pmatrix} = 0$$

$$K(x, y) = \frac{(\partial^2 U/\partial x^2)(\partial^2 U/\partial y^2) - (\partial^2 U/\partial x\,\partial y)^2}{[1 + (\partial U/\partial x)^2 + (\partial U/\partial y)^2]^2}$$

Thus, the instability of the motion can be related to the sign of the curvature of the potential energy surface, i.e., instability corresponds to a negative curvature. This implies that with the knowledge of the surface map of the potential energy one can qualitatively define the conditions for which the motion becomes unstable. That is, if a particle in its motion passes through a region with negative curvature of the potential energy, then in that region the stability of the motion is violated and, therefore, regular motion can change to chaotic.

Dynamic chaos in the motion of charged particles through a crystal

Akhiezer A.I., V.I. Truten’, Shul’ga N.F. Dynamic chaos in the motion of charged particles through a crystal // Phys. Rep. (Review Section of Physics Letters). 1991. Vol. 203, № 5. P. 289–343.

$$\mathscr{E}_{\perp} = \tfrac{1}{2} E\dot{\rho}^{2} + U(\rho)$$

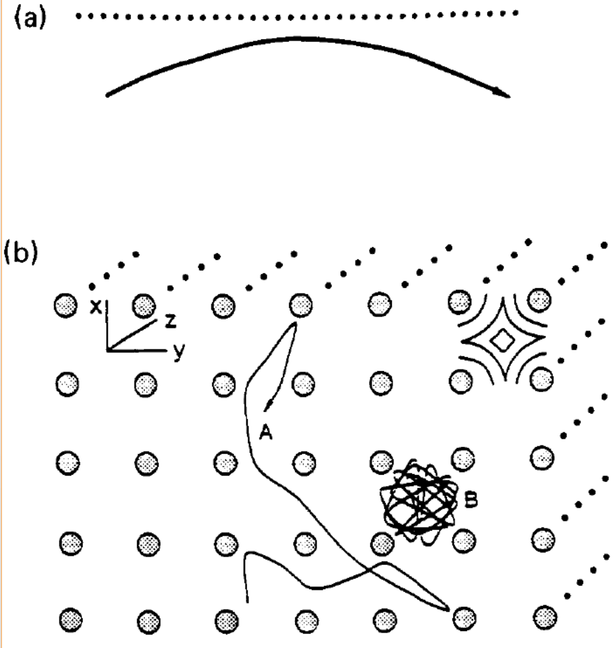

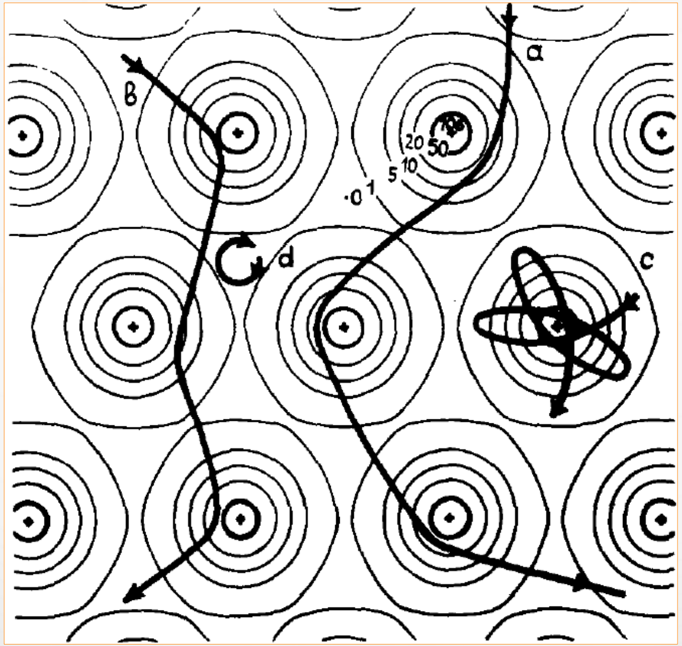

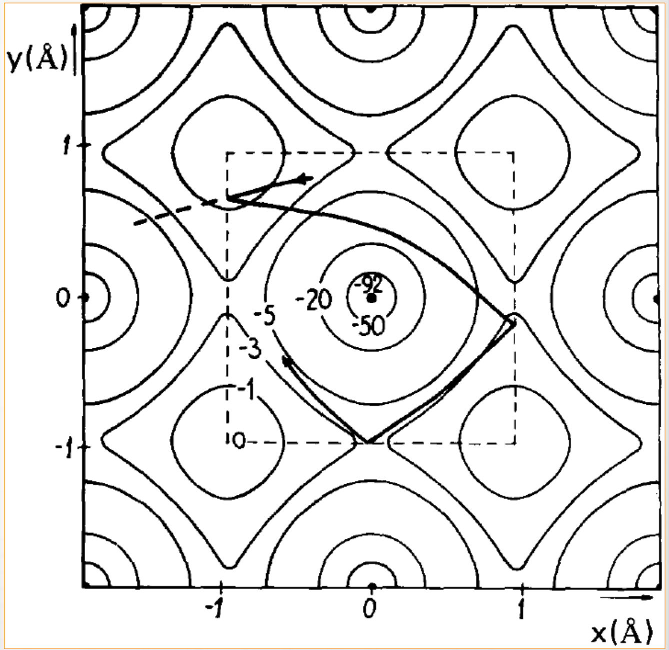

Turning a beam of high-energy charged particles by means of scattering by atomic rows of a curved crystal

Grinenko A.A., Shul’ga N.F. Turning a beam of high-energy charged particles by means of scattering by atomic rows of a curved crystal // J. Exp. Theor. Phys. Lett. 1991. Vol. 54. P. 524.

$$\theta_{x,i+1} = \theta_{x,i} \cos \varphi_i + \theta_{y,i} \sin \varphi_i,$$

$$\theta_{y,i+1} = \theta_{y,i} \cos \varphi_i - \theta_{x,i} \sin \varphi_i - \frac{\tau_i V_{11i}}{R},$$

$$\psi_{i+1} = (\theta^2_{x,i+1} + \theta^2_{y,i+1})^{1/2},$$

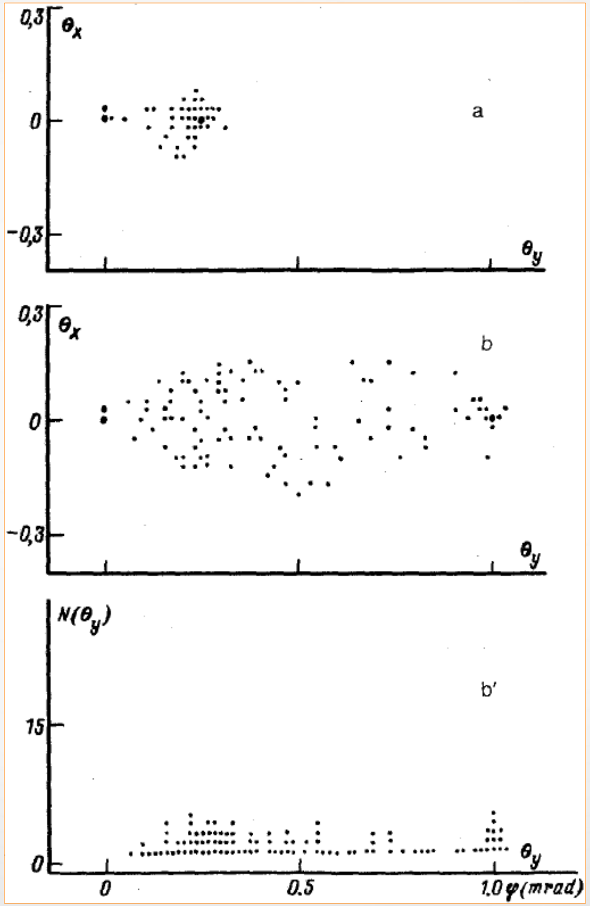

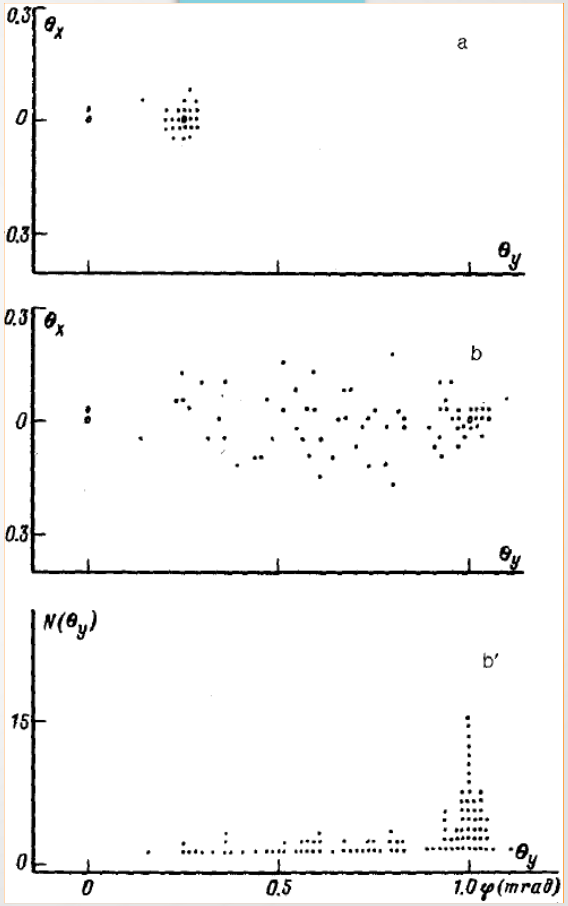

Multiple scattering of ultrahigh-energy charged particles on atomic strings of a bent crystal

Shul'ga N.F., Greenenko A.A. Multiple scattering of ultrahigh-energy charged particles on atomic strings of a bent crystal // Phys. Lett. B. 1995. Vol. 353, № 2. P. 373–377.

$$\overline{\psi^2} = \frac{lL}{R^2} \leq \psi_c^2$$

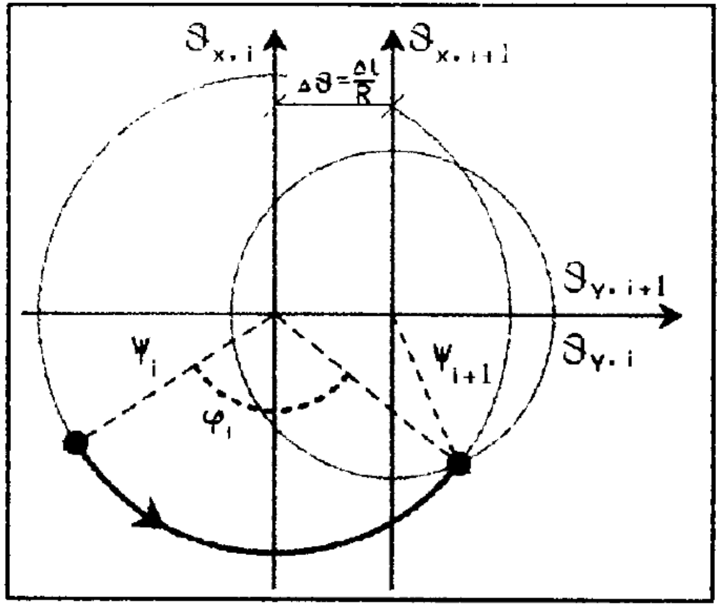

Fig. 1. Particle's angular coordinates change under transit from one axis to another.

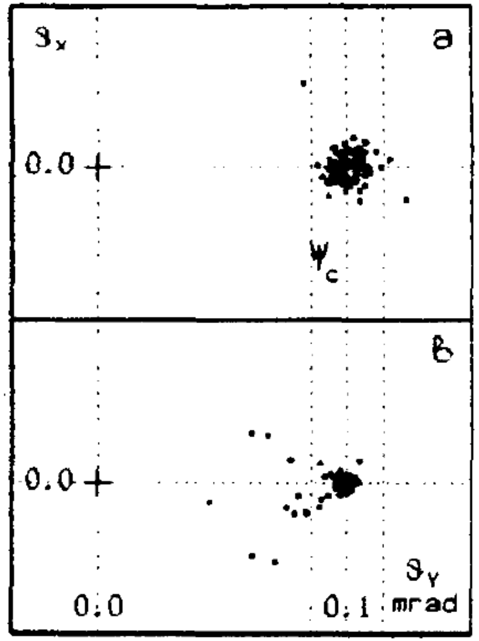

Fig. 2. Angular distributions of negative (a) and positive (b) charged particles with energy $\varepsilon = 800$ GeV, which pass through bent SI crystal with $R = 3\times10^4$ cm, $L = 3$ cm near axis $\langle 111 \rangle$. The initial particle angular coordinates are $(\vartheta_x, \vartheta_y) = (0, 0)$.

Multiple scattering of ultrahigh-energy charged particles on atomic strings of a bent crystal

Baurichter A. et al. New results from the CERN-SPS beam deflection experiments with bent crystals // Nucl. Instrum. Meth. B. 1996. Vol. 119, № 1. P. 172–180.

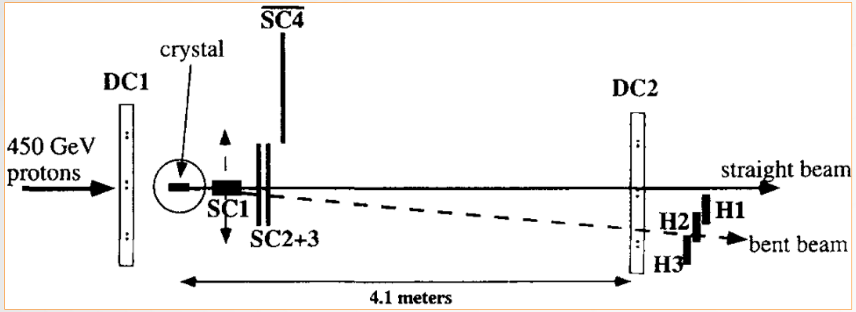

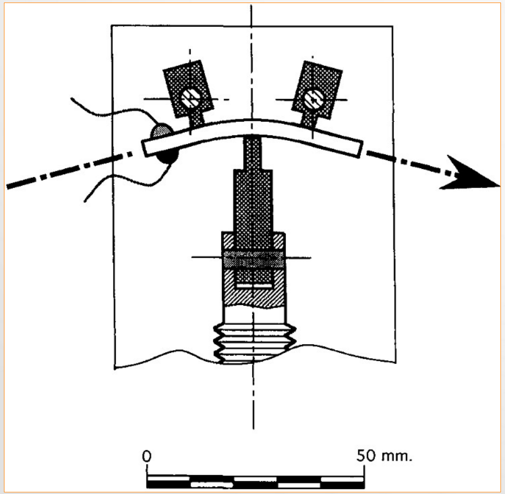

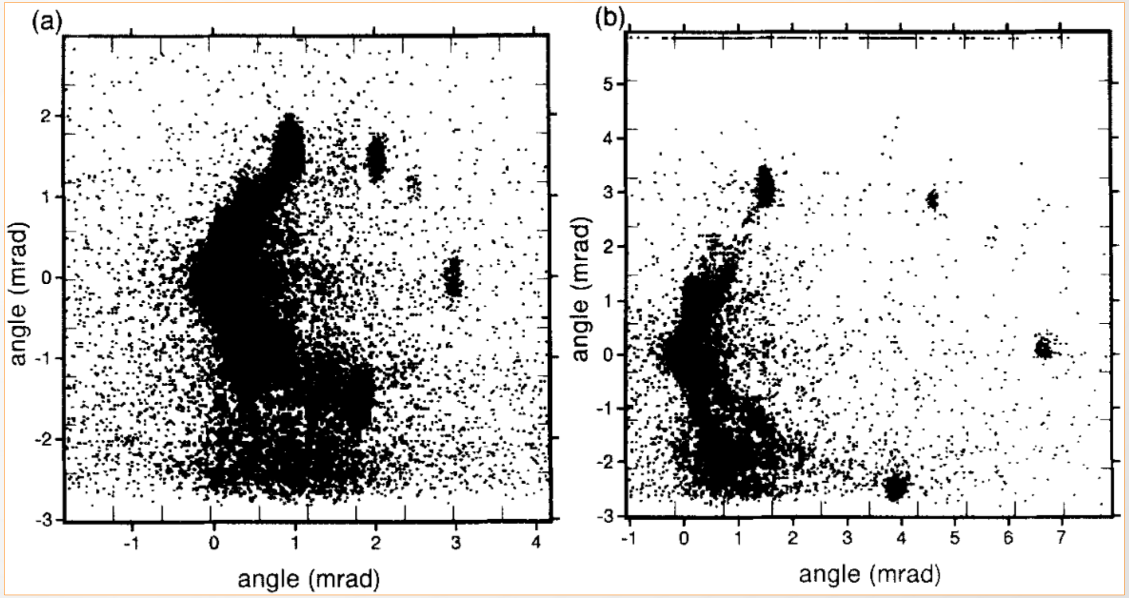

450 GeV / c protons

Multiple scattering of ultrahigh-energy charged particles on atomic strings of a bent crystal

Greenenko A.A., Shul'ga N.F. Experimental verification of the doughnut scattering mechanism of a high-energy beam deflection by a bent crystal // Phys. Lett. B. 1999. Vol. 454, № 1. P. 161–164.

$$\alpha = \frac{L}{R\psi_c} \cdot \frac{l_\perp}{R\psi_c} < 1, \qquad (1)$$

$$\frac{l_\perp}{R\psi_c} < 1 \qquad (2)$$

The parameters of the experiment [1] satisfied the inequality (2).

Note, however, that the condition Eq. (1) in comparison to Eq. (2) contains an additional factor $(L/R\psi_c)$, which invalidates the bending condition (1) in the case of the experiment [1]. Namely, the parameter α values for [1] are: $\alpha_{p^+} \approx 83$ for protons and $\alpha_{\pi^-} \approx 83$ for pions.

The results of the experiment [1] have demonstrated that in the case of positively charged particles a small part of the beam follows the bent axis, while in the case of negatively charged particles the bending was absent.

Multiple scattering of ultrahigh-energy charged particles on atomic strings of a bent crystal

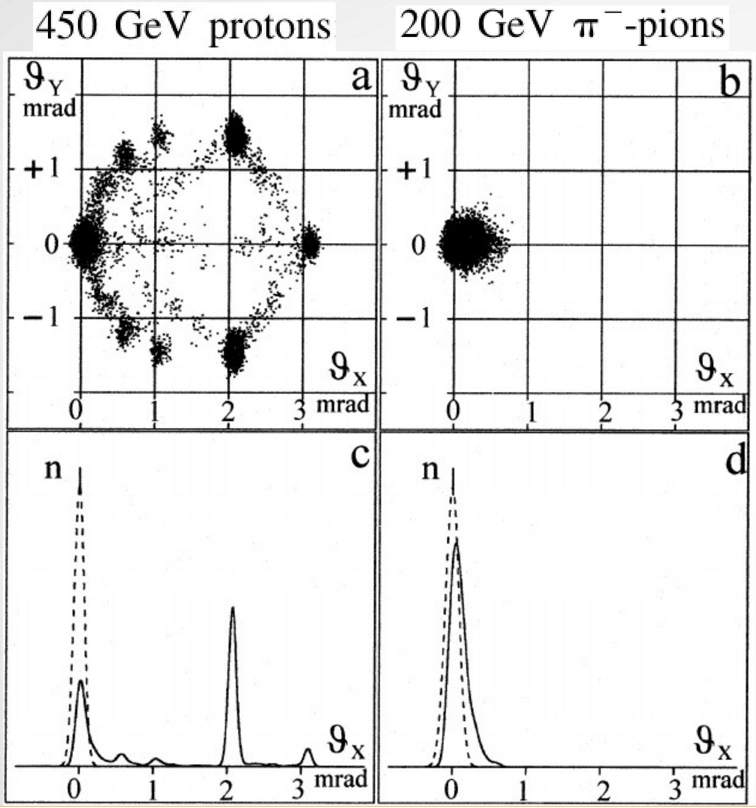

Beam passage through a bent silicon crystal with length 3.1 cm and curvature radius 10 m near the <110> axis

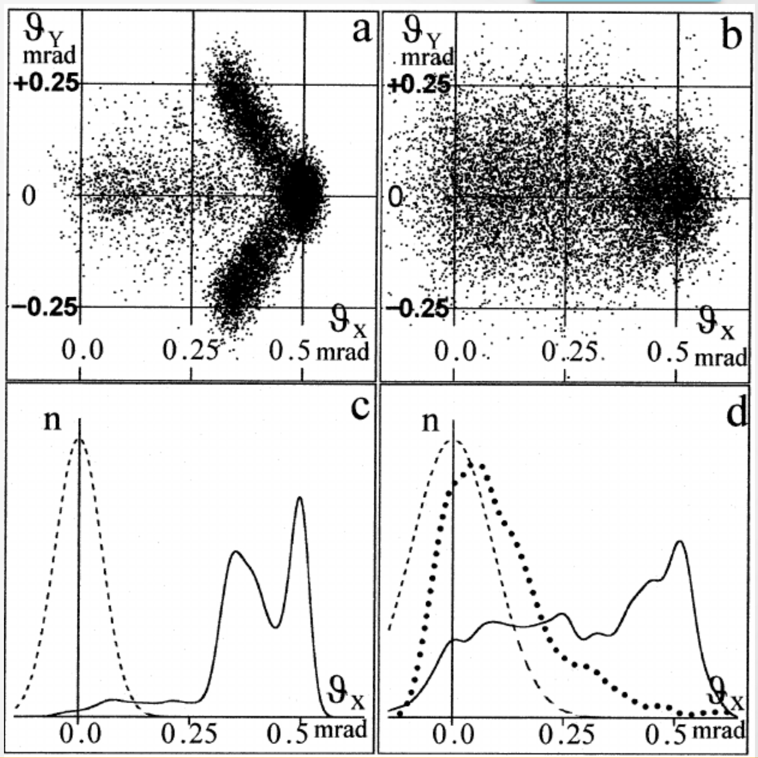

Beam passage through a bent silicon crystal with length 10 cm and curvature radius 200 m near the <110> axis

Experimental confirmation

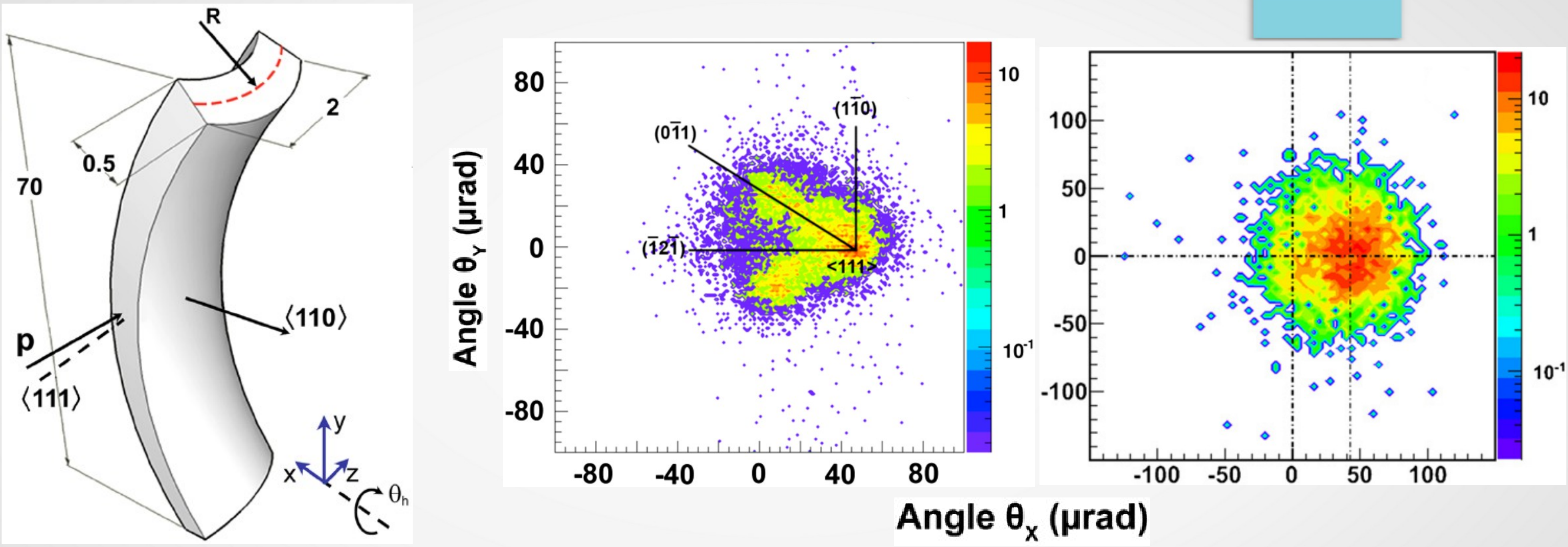

Scandale W., Vomiero A., Baricordi S. et al. High-efficiency deflection of high-energy protons through axial channeling in a bent crystal. Phys. Rev. Lett. 2008. Vol. 101, No. 16. P. 164801.
Scandale W., Vomiero A., Bagli E. et al. High-efficiency deflection of high-energy negative particles through axial channeling in a bent crystal. Phys. Lett. B. 2009. Vol. 680, No. 4. P. 301–304.

Probability of close collisions

p, E=270 GeV,
Si <110>, (110),
L = 5 mm,
R = 5 m

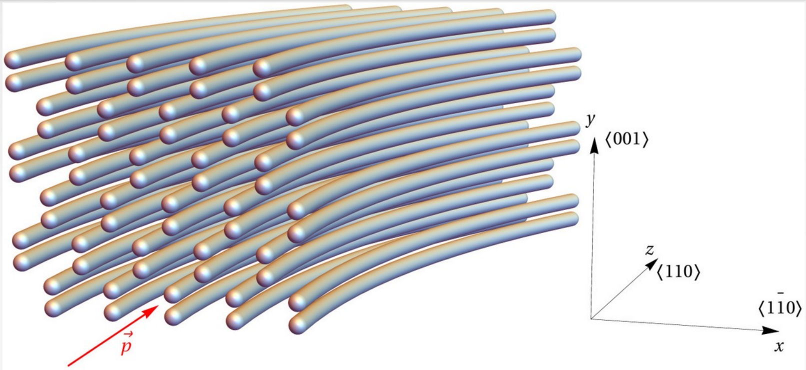

$$w_a = \frac{4\pi r_T^2}{a_x a_y} = 4\sqrt{2}\pi r_T^2/a^2 \approx 3.39 * 10^{-3}$$

$$w_p = \frac{4r_T}{a_x} = 4\sqrt{2}r_T/a \approx 78.12 * 10^{-3}$$

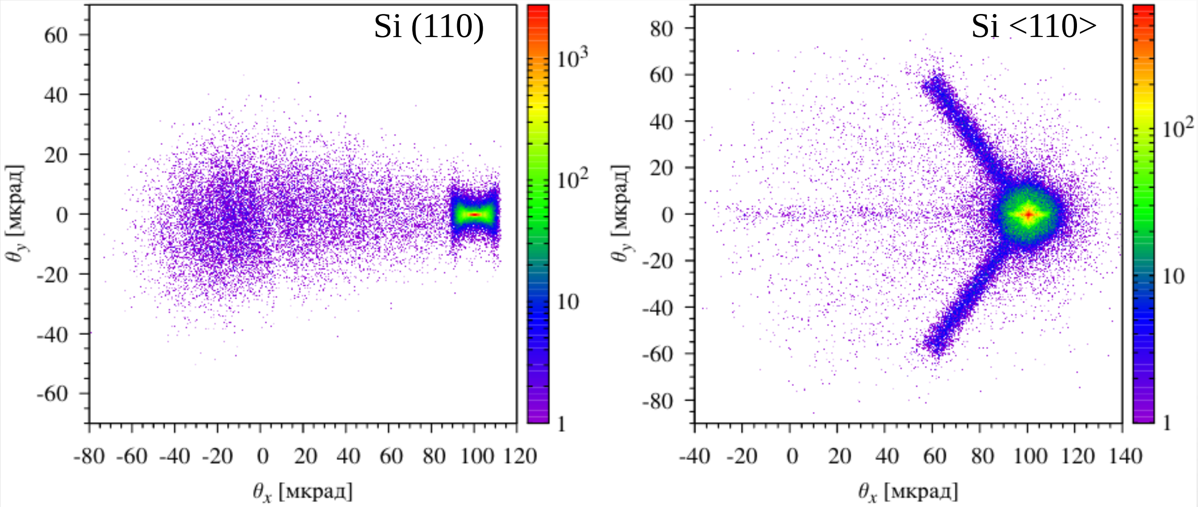

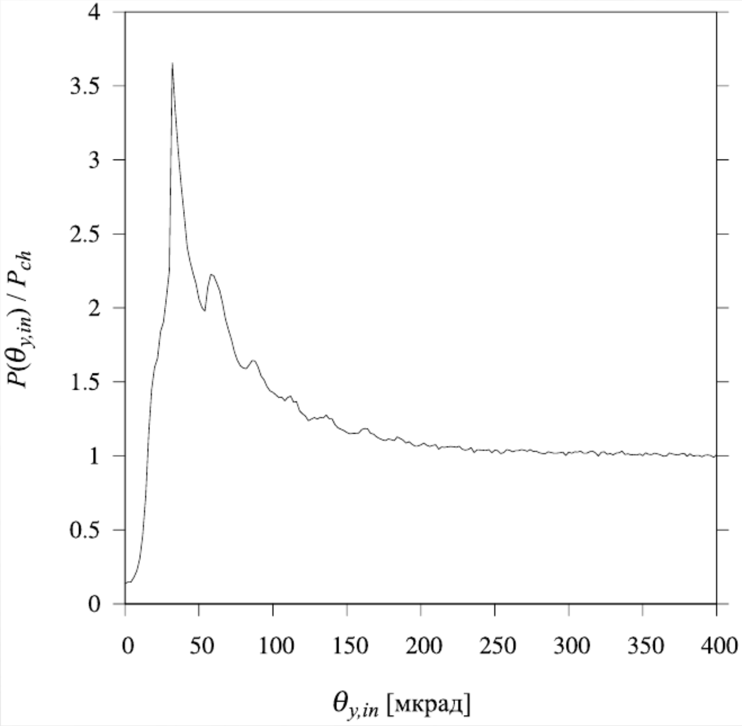

Chesnokov Yu.A., Kirillin I.V., Scandale W. et al. Phys. Lett. B. 2014. Vol. 731. P. 118–121.

Probability of close collisions

Scandale W., Arduini G., Butcher M. et al. Phys. Lett. B. 2016. Vol. 760. P. 826–831.
Scandale W., Andrisani F., Arduini G. et al. Eur. Phys. J. C. 2018. Vol. 78, No. 6. P. 505.

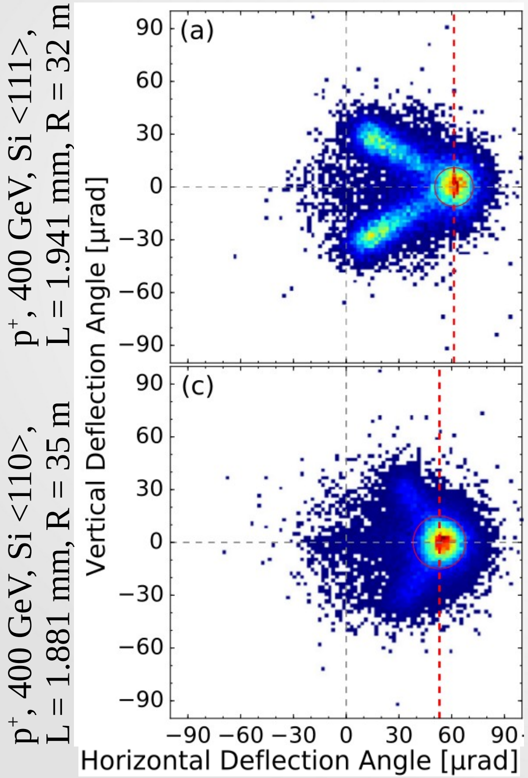

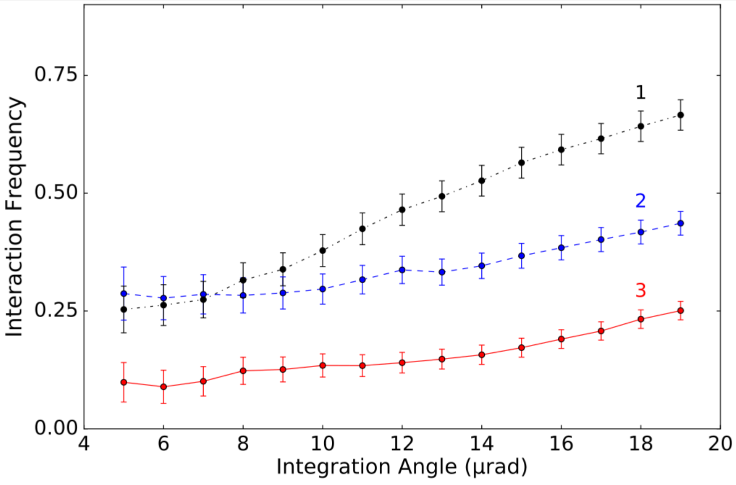

Fig. 5. Measured inelastic nuclear interaction (INI) frequency of 400 GeV/c protons interacting with the ⟨111⟩ and ⟨110⟩ crystals as a function of the angular region around the (110) planar channeling (black dash-dotted line, 1), the ⟨111⟩ axial channeling (blue dashed line, 2) and ⟨110⟩ (red continuous line, 3) orientations. The values are normalized to the INI frequencies for the amorphous crystal orientation. (For interpretation of the references to color in this figure legend, the reader is referred to the web version of this article.)

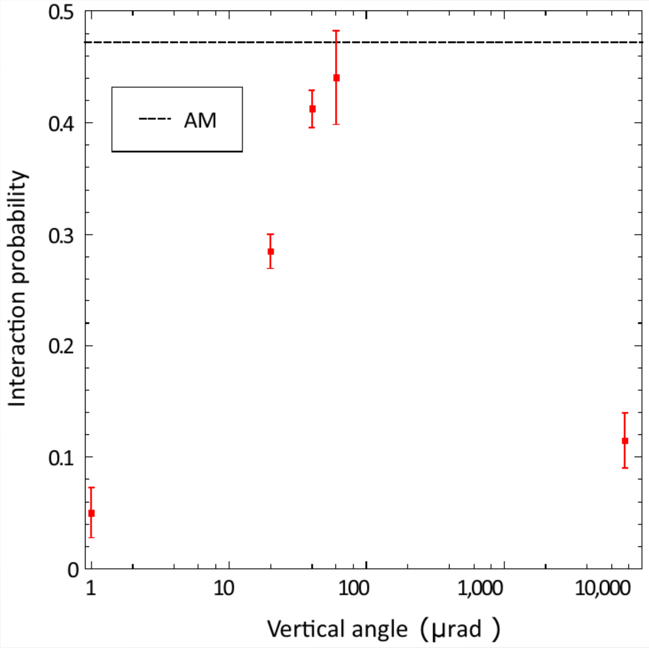

Optimal radius of curvature (stochastic deflection)

$$\langle\psi^2\rangle = \frac{lL}{R^2} \le \psi_c^2 \qquad \overline{\Psi_{inc}}^2 = \xi L \qquad L_{st} = \frac{\psi_m^2}{l/R^2+\xi} \qquad \alpha_{st} = \frac{L_{st}}{R} = \frac{\psi_m^2}{l/R+\xi R}$$

π^-, E=150 GeV, Si <110>

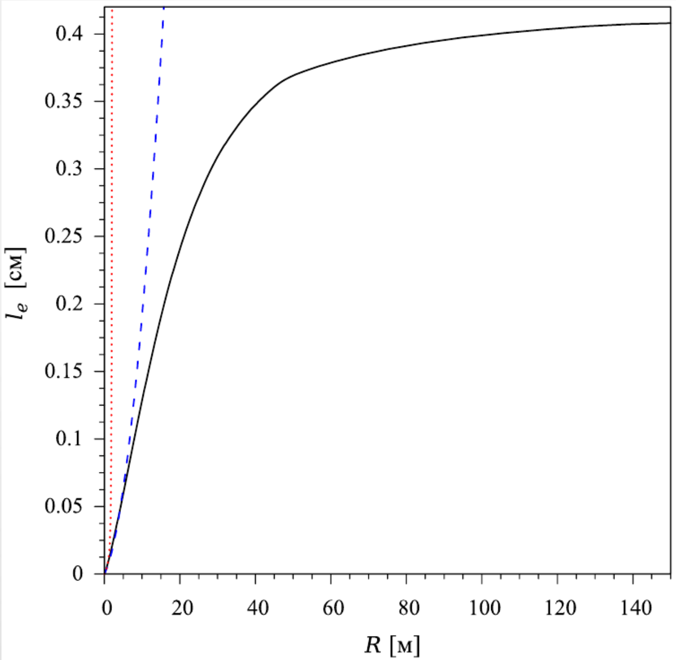

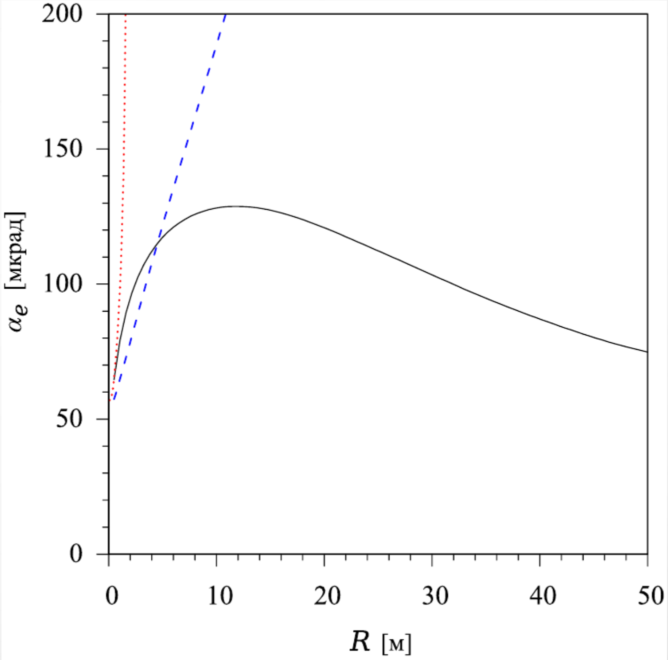

Kirillin I.V., Shul'ga N.F., Bandiera L. et al. Eur. Phys. J. C. 2017. Vol. 77. P. 117 (1–7).

Optimal radius of curvature (stochastic deflection)

$$\overline{\psi_{inc}^2} = \zeta L/E^2 \Rightarrow \alpha_{st} = \frac{\psi_m^2}{l/R + \zeta R/E^2} \Rightarrow R_{opt} = E\sqrt{l/\zeta}$$

$$l \approx \frac{1}{4nda}\sqrt{\frac{E}{U_0}} \Rightarrow R_{opt} \propto E^{5/4}$$

$$\psi_m \approx 1,5\psi_c \propto E^{-1/2} \Rightarrow \max(\alpha_{st}) = \frac{\psi_m^2}{l/R_{opt} + \zeta R_{opt}/E^2} \propto E^{-1/4}$$

π^-, Si <110>

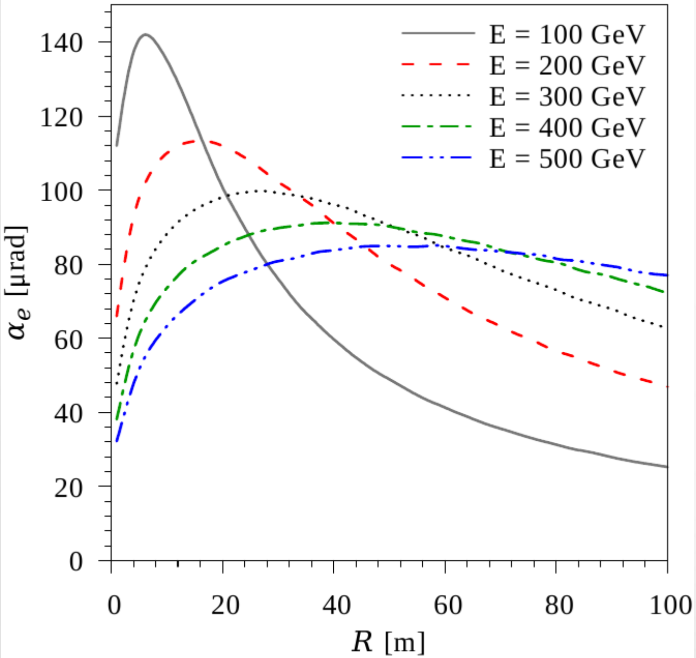

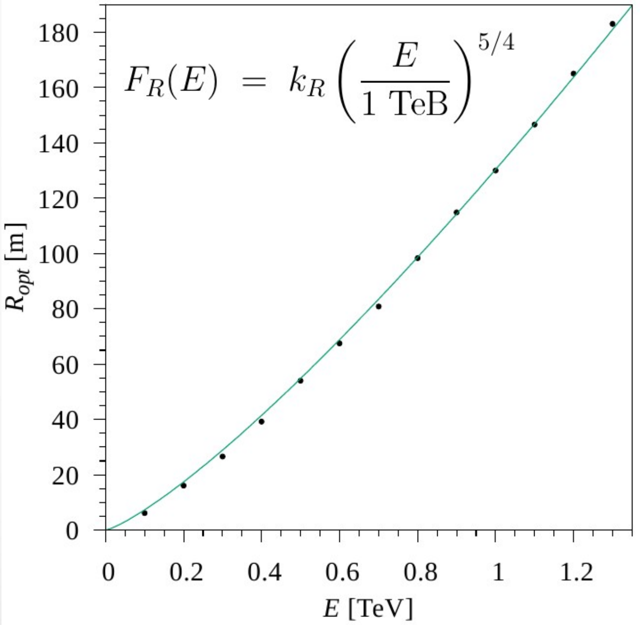

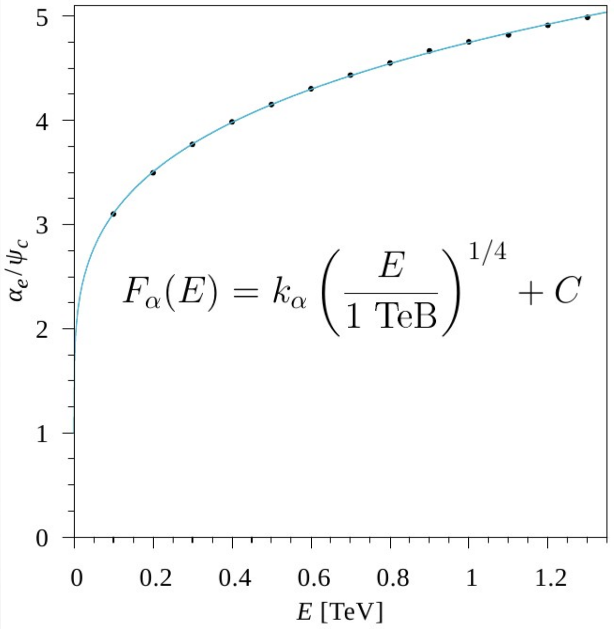

Kirillin I.V. Probl. Atom. Sci. Tech. 2017. Vol. 109. № 3. P. 67–71

$k_R \approx 130$ м

$k_\alpha \approx 3,75$ і $C \approx 1$

Optimal radius of curvature (planar channeling)

$$U_{\mathrm{eff}}(x) = U_{\mathrm{p}}(x) + Ex/R$$

$$\left.\frac{dU_{\mathrm{eff}}(x)}{dx}\right|_{x=x_0} = 0$$

$$R_{\mathrm{c}} = \frac{E}{|U'_{\mathrm{p}}(x_0)|}$$

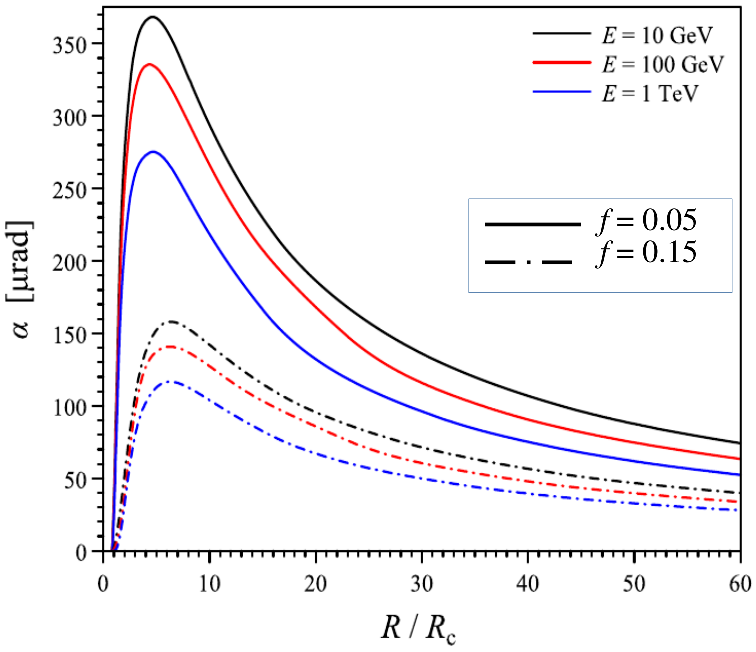

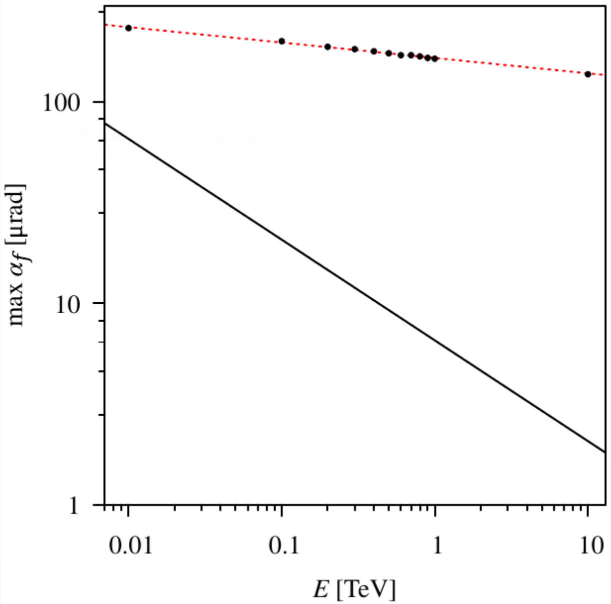

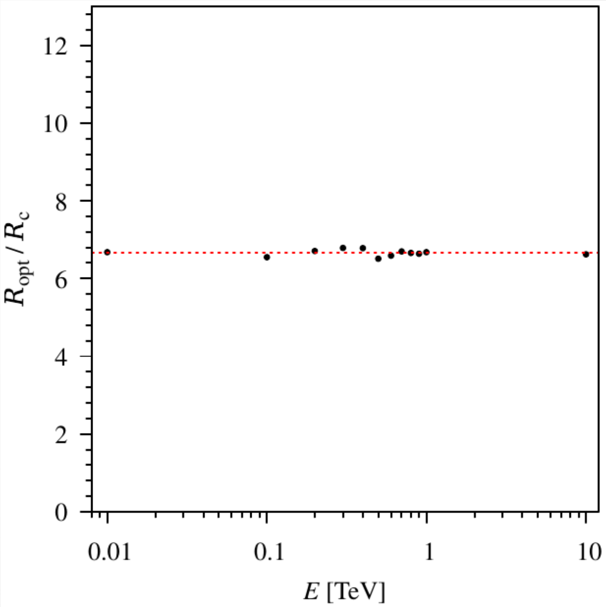

Kyryllin I.V., Shul'ga N.F. Eur. Phys. J. C. 2019. Vol. 79. P. 1015 (1–6).

A. Sytov, G.Kube, L. Bandiera et al. First design of a crystal-based extraction of 6 GeV electrons for the DESY II Booster Synchrotron

Eur. Phys. J. C (2022) 82:197

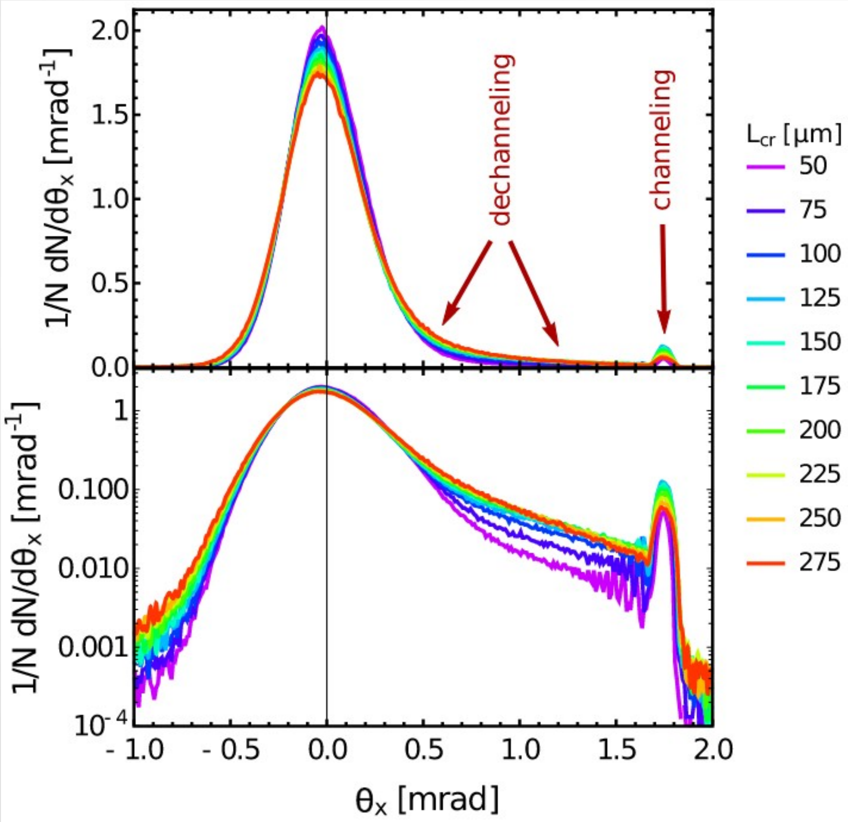

single-turn

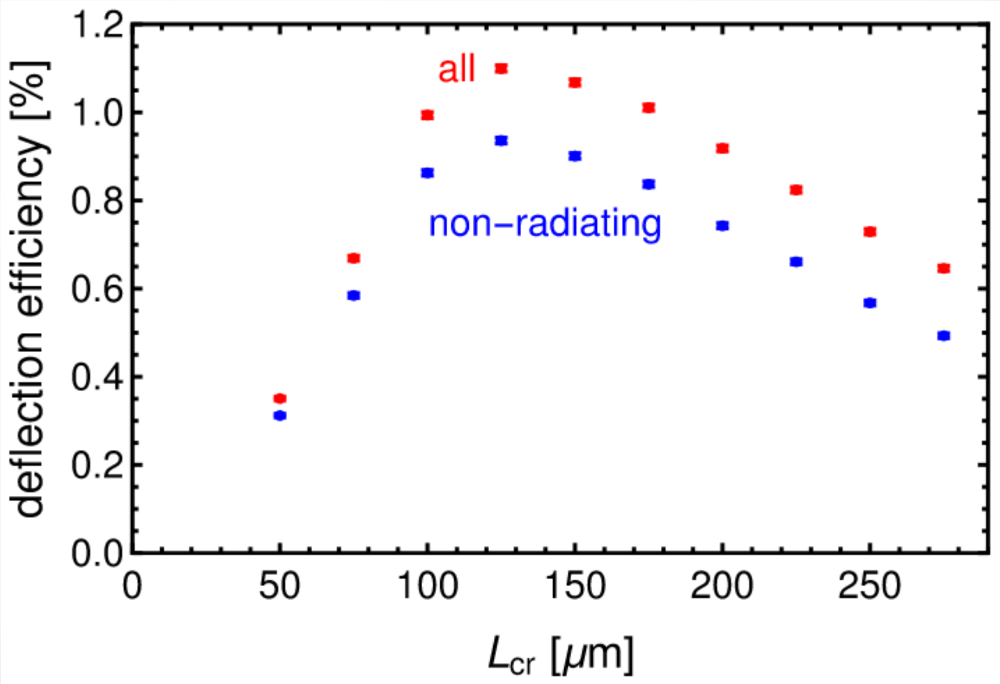

A. Sytov, G.Kube, L. Bandiera et al. First design of a crystal-based extraction of 6 GeV electrons for the DESY II Booster Synchrotron

Eur. Phys. J. C (2022) 82:197

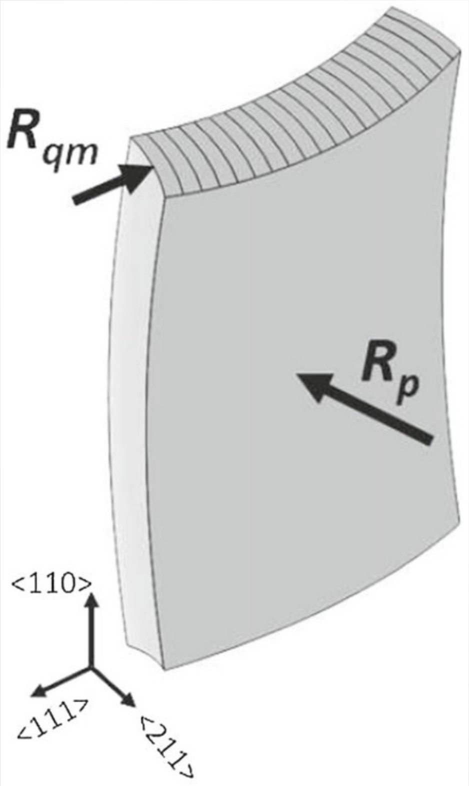

multi-turn

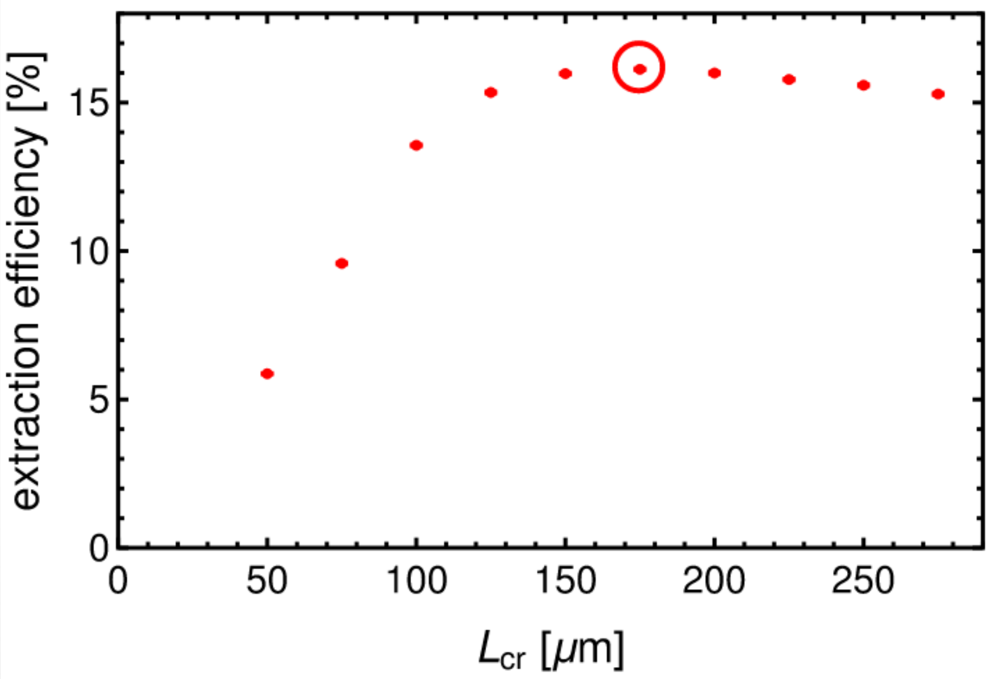

L = 175 µm,

α = 1.75 mrad

R = L / α = 10 cm

Dependence of deflection angle on R (α = 2 mrad)

(111) plane

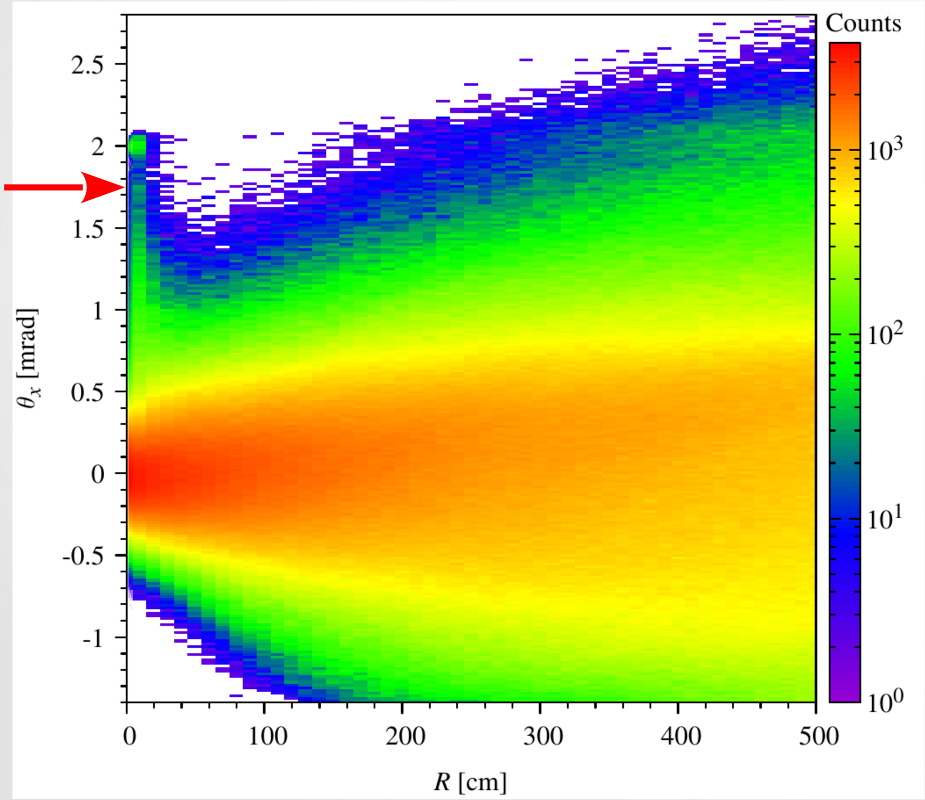

(110) axis

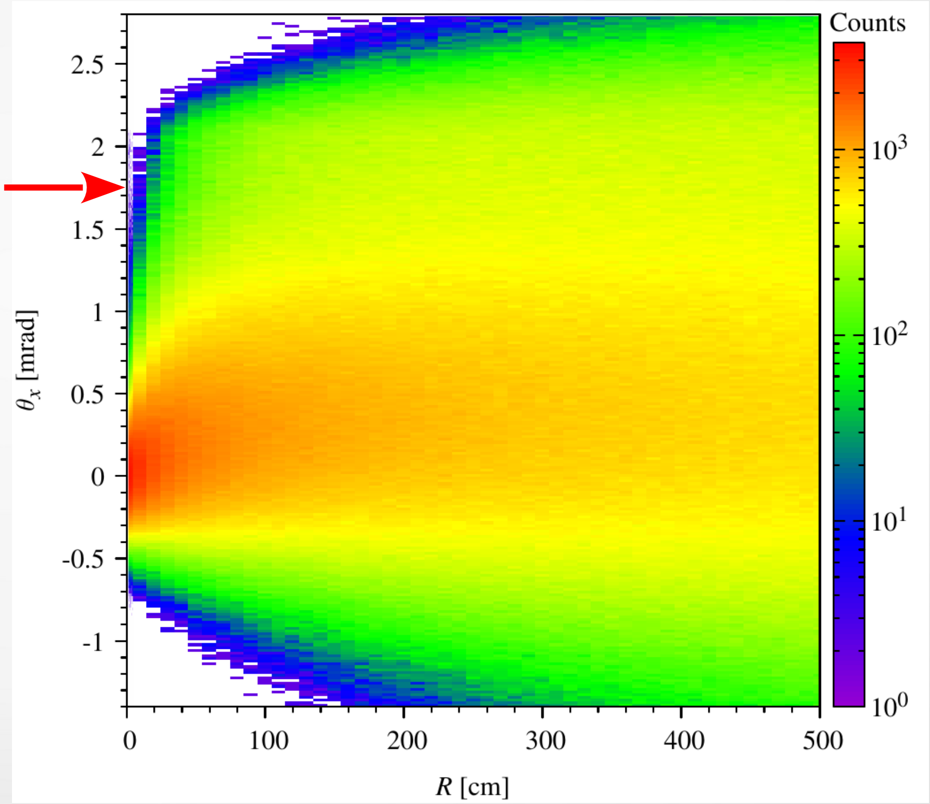

R = 8 cm (α = 2 mrad, L = 160 µm)

(111) plane

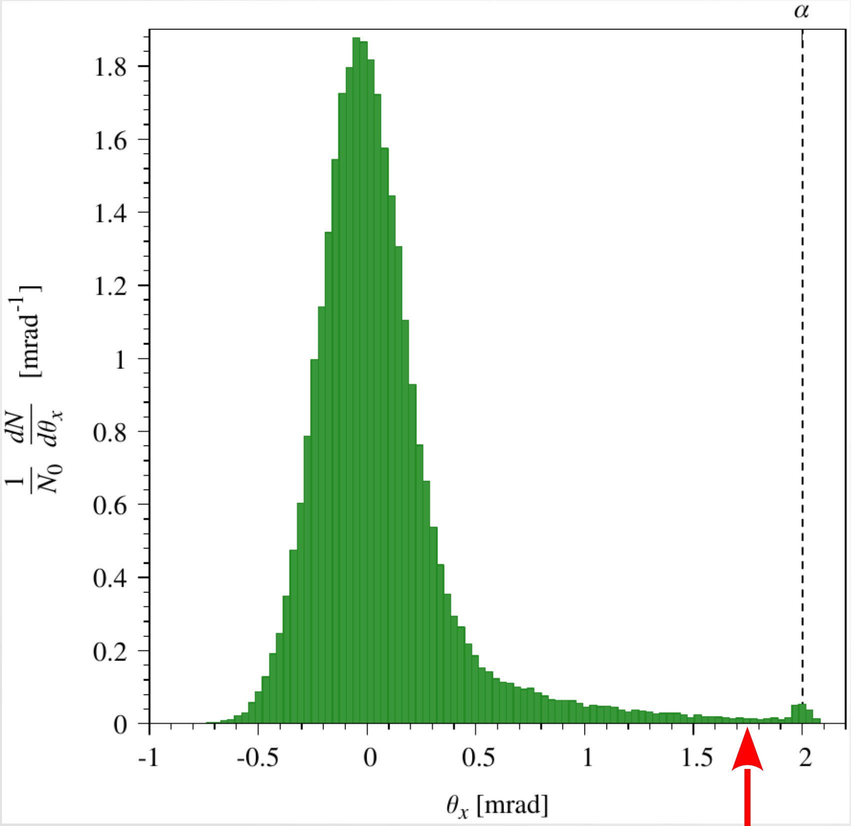

(110) axis

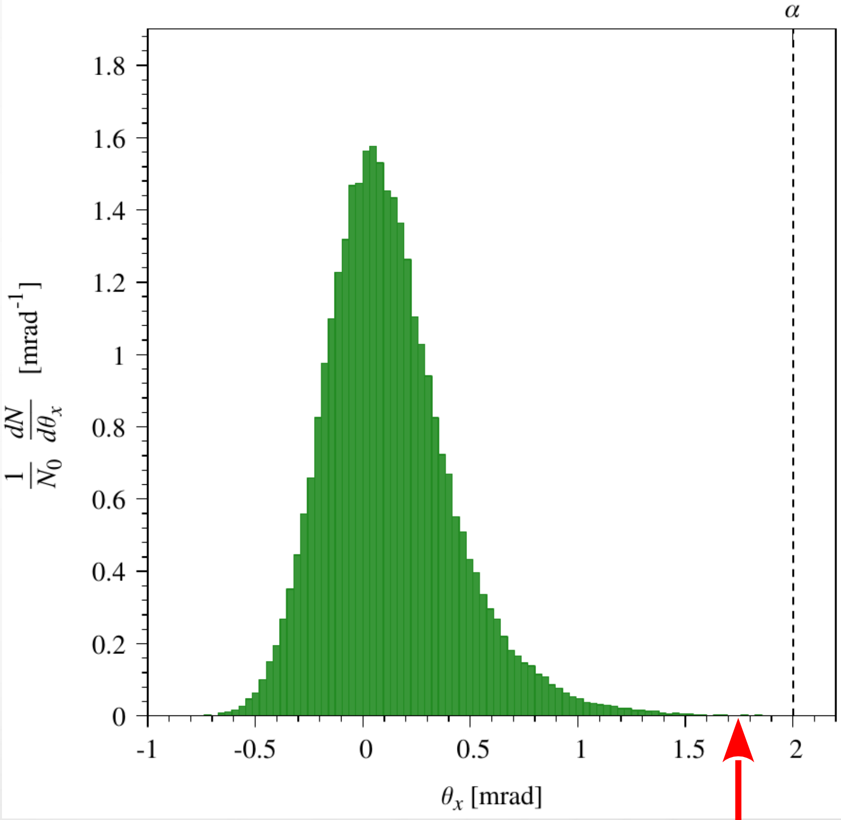

R = 1 m (α = 2 mrad, L = 2 mm)

(111) plane

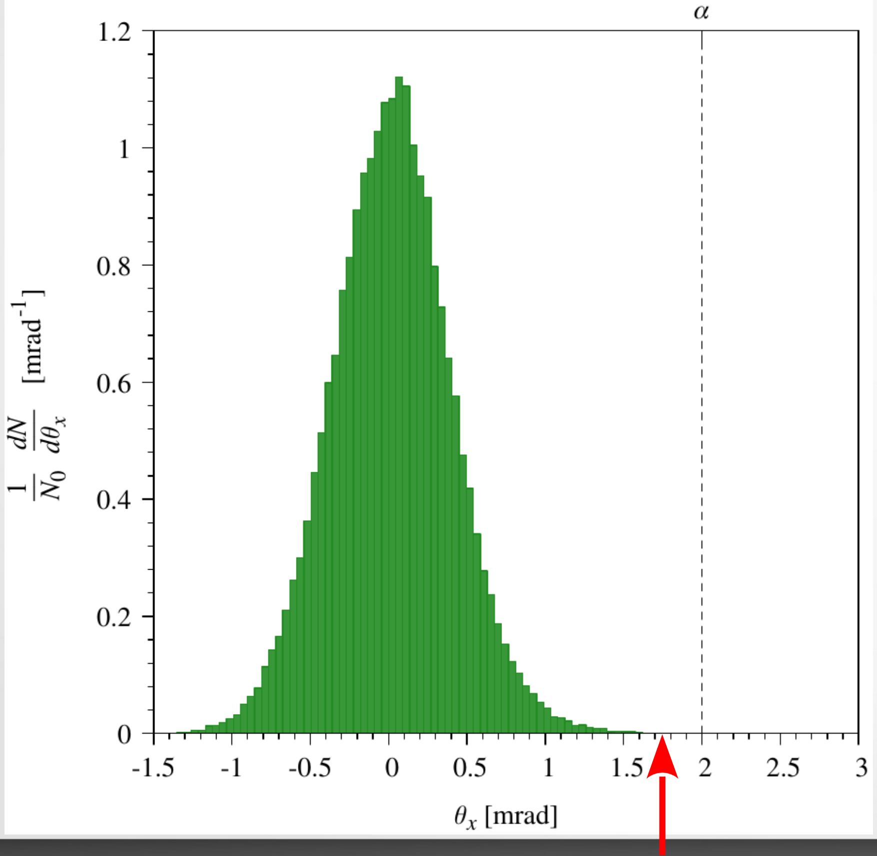

(110) axis

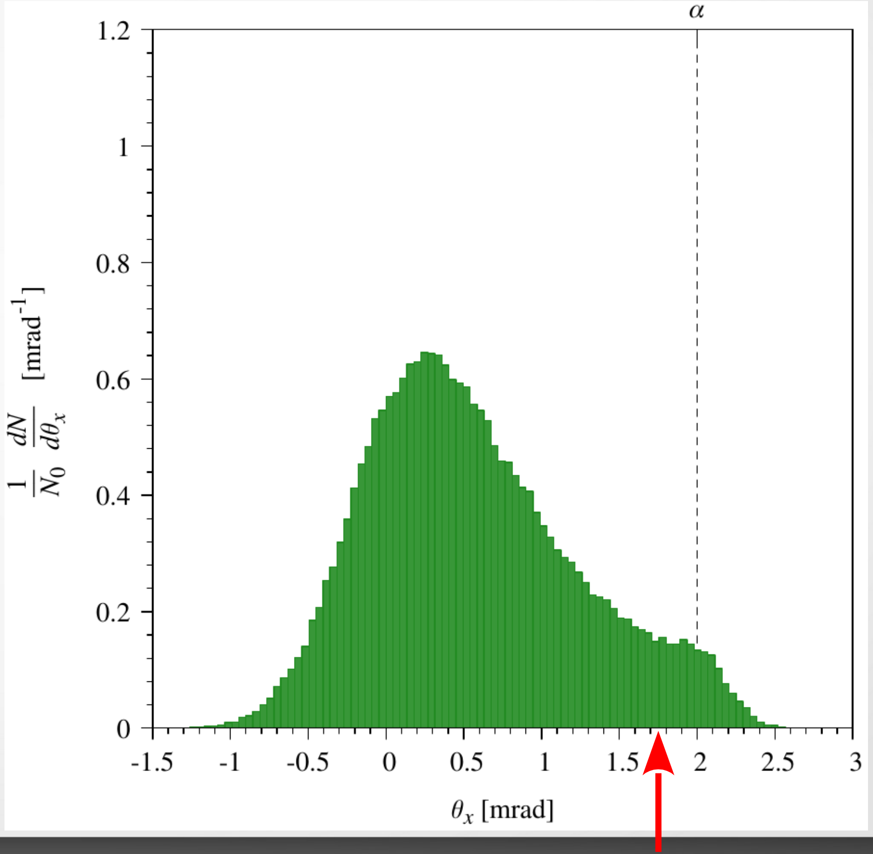

R = 5 m (α = 2 mrad, 1 cm)

(111) plane

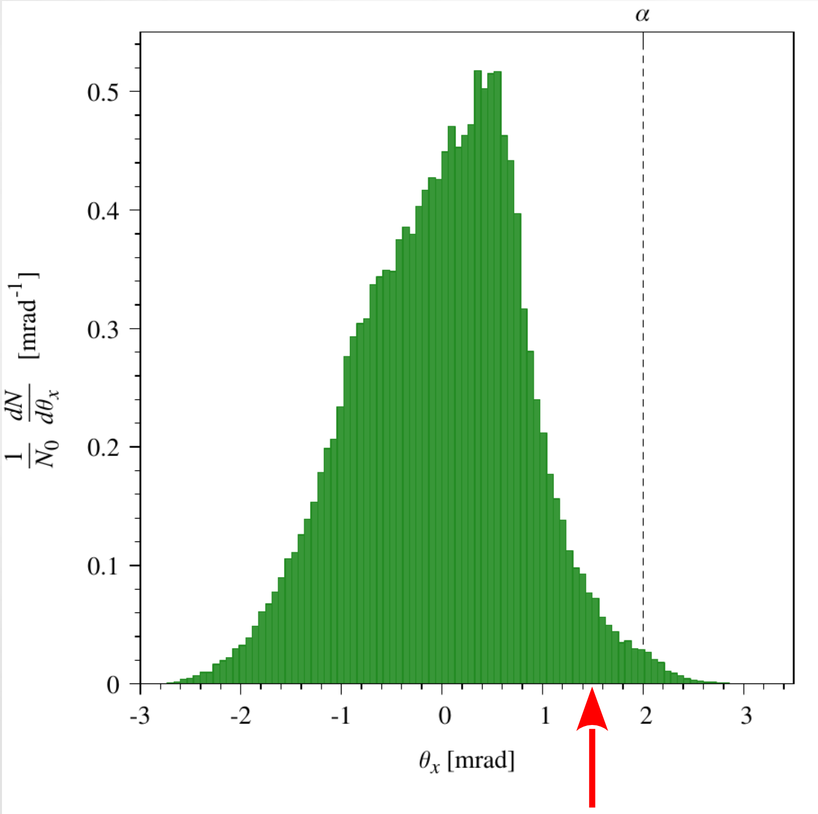

(110) axis

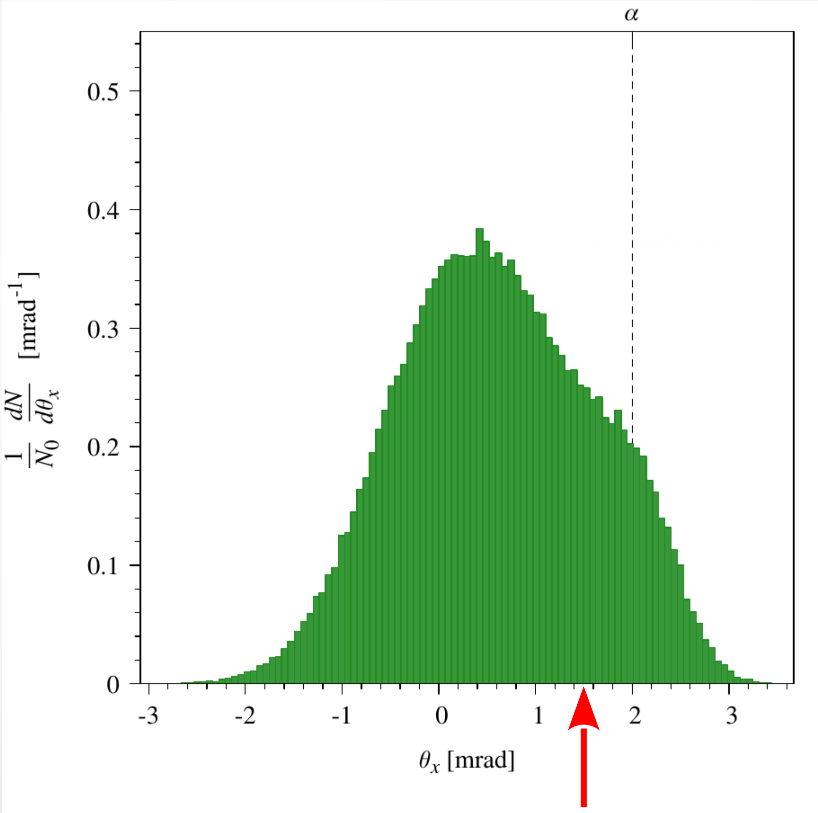

Deflection efficiency. $\theta_x > 1.75$ mrad

(111) plane

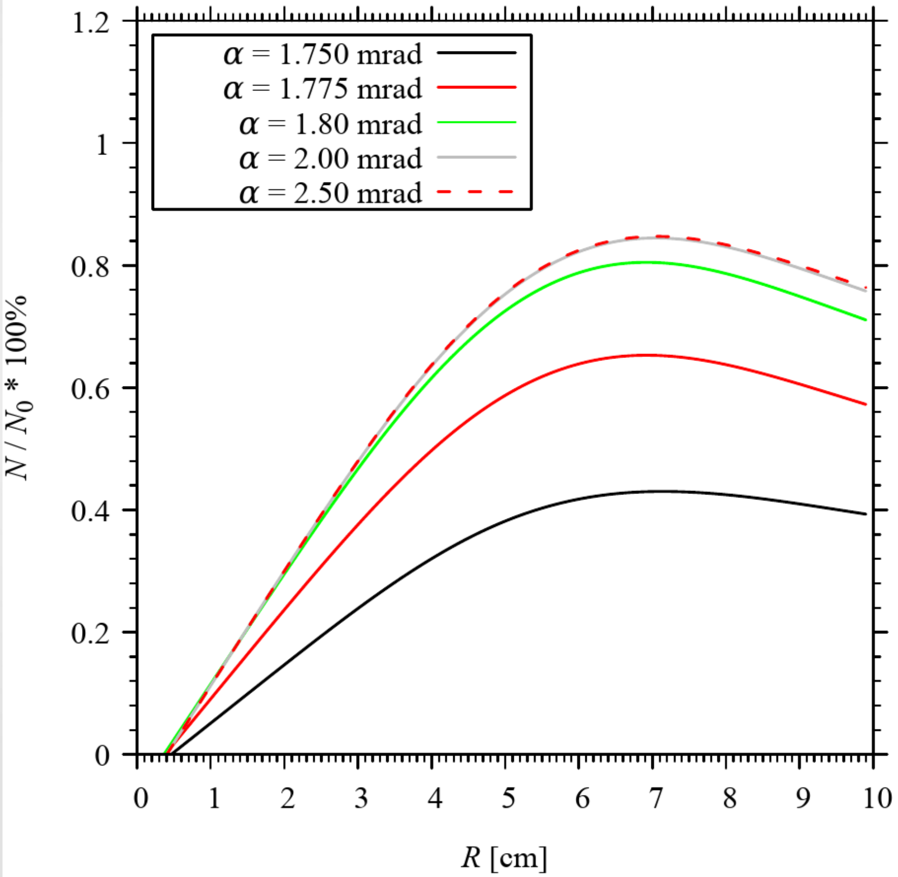

(110) axis